IN-05-CR

73910

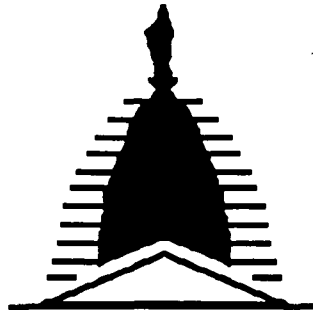*P.104*

UNIVERSITY of NOTRE DAME

NASA/USRA UNIVERSITY ADVANCED DESIGN PROGRAM 1990-1991

UNIVERSITY SPONSOR
BOEING COMMERCIAL AIRPLANE COMPANY

FINAL DESIGN PROPOSAL

THETA GROUP - THE HOTBOX

A Proposal in Response to a Commercial Air Transportation Study

May 1991

Department of Aerospace and Mechanical Engineering
University of Notre Dame
Notre Dame, IN 46556

EXECUTIVE SUMMARY   *1.04 miles ?*

The *Hotbox* is a 40 passenger commercial aircraft designed to have a minimum range of 5500 ft, and cruise at a velocity of 30 ft/sec. The aircraft is designed to serve the longer range overseas market in Aeroworld.

The driving force behind the design was to generate the greatest possible return on investment and profit for an Aeroworld airline. This goal, at least in an underlying sense, influenced all aspects of the design. Due to the seven week engineering time frame, ease of construction and simplicity of design also had a primary influence on the design. In addition, space restrictions (disassembled aircraft must fit in a 2'x3'x5' box) imposed significant limitations on aircraft design.

From these primary design goals, a set of secondary drivers evolved. First, in order to serve all the airports in the overseas market the *Hotbox* was required to be able to utilize a five foot gate. A weight requirement was set a 4.5 lbs in order to maximize aircraft efficiency. Finally, a single engine system was chosen because it minimized system weight, complexity, and cost. From these primary and secondary design goals, the *Hotbox* was born.

The *Hotbox* is estimated to cost $152,000 Aeroworld dollars (AD) and will sell for $200,000 (AD). A ticket price of $38 flat rate + $9.70 per 50 ft is recommended. This ticket price is, on an average flight, 15% higher than the ticket cost of a ship. Due to the time savings involved with air travel, this excess cost is considered acceptable. A market consisting of 27 routes and 316 flights per day is estimated to generate a $42.3 Million (AD) net income and a 53.8% annual return on investment.

The propulsion system for the *Hotbox* consists of a nose mounted Astro 15 electric powered motor and a Top Flight 12-6 propeller. The system

is powered by nine 1.2 V, 1200 mah batteries. Early in the design process, studies indicated that the Astro 15 motor would provide sufficient power for all phases of the mission and better cruise performance than other motors considered. After ordering this motor, however, weight considerations became an increasing concern in the design of the *Hotbox*. The Top Flight 12-6 was utilized because it allowed for minimum battery weight, and was the only propeller considered that met the 60 ft takeoff requirement.

A Spica airfoil was selected for the *Hotbox* based on the ease of construction of its flat bottom and its positive lift and drag characteristics. In order to provide acceptable wing loading, the *Hotbox* has a wing area of 7.33 ft^2. Aircraft aspect ratio is 8.72. To simplify construction, no sweep, taper or twist was incorporated into the wing design. The wing consists of a spar and rib construction with a Monokote skin. In order to fit into the five foot gates of Aeroworld, the *Hotbox*'s 8 ft wing must be hinged. The primary hinge mechanism will be enclosed in the wing and located at the quarter chord and 26.75 in. from the fuselage centerline.

A fuselage of rectangular cross-section will internally contain the propulsion system, control system and a passenger bay with 2x20 seating. The center of gravity is located at 30.0% chord with the aircraft fully loaded and at 21.5% chord without passengers.

A combination of directional and longitudinal control will enable the *Hotbox* to maneuver. In order to reduce the complexity of the design and to reduce servo weight, ailerons were not utilized. Flat plates were used in both the horizontal and vertical tails in order to further simplify construction. The aircraft will turn using a combination of rudder deflection and dihedral. A static margin of 5-10% mean aerodynamic chord is typical for conventional

aircraft. A static margin of 15% was used in the *Hotbox* to allow for the longer response time involved with its ground based pilot.

The final design of the *Hotbox* provides for takeoff distance in 26.5 ft and normal cruise range of 17,000 ft. Maximum range and maximum endurance for the aircraft are 20,600 ft. and 14.3 min. respectively. The estimated normal turning radius is 48.4 ft. assuming a 30° bank angle.

Key Design Information

AERODYNAMICS

Wing Area	7.33 ft^2
Aspect Ratio	8.72
Chord	11 in
Span	8 ft
Taper Ratio	1
Sweep	0°
Dihedral	7°
C_{do}	0.034
Airfoil Section	Spica
Wing mount angle	5°

PERFORMANCE

Takeoff distance	26.5 ft
Velocity at takeoff	25.5 ft/sec
Velocity in cruise	30 ft/sec
Range (cruise)	17000 ft
Endurance (cruise)	10 min
Max Range	20606 ft
Max Endurance	14.3 min
Max Rate of Climb	10 ft/sec
Turn Radius	48.4 ft

EMPENEGE

Horiz. & Vert. Tail airfoil sections	Flat plate
Horiz. Tail area	1.01 ft^2
Elevator area	.10 ft^2
Elevator max deflection	± 15°
Vertical Tail area	.42 ft^2
Rudder area	.29 ft^2
Rudder max deflection	± 20°

PROPULSION

Engine	Astro 15
Propeller	Top Flight 12-6
Number of Batteries	9
Battery pack voltage	10.8 V
Battery capacity	1200 mah
Cruise gear RPM	6300

STRUCTURE

Weight	68.6 oz.
Fuselage length	57.0 in.
Fuselage width	5.5 in.
Fuselage height	2.75 in.

ECONOMICS

Ticket cost	$38+9.70 per 50 ft
Aircraft production cost	$152,000
Aircraft sales price	$200,000

The Hotbox

12"

7.125"

20.8"

11"

6"

10"

57"

5.5"

48"

TABLE OF CONTENTS

1. MISSION DEFINTION

1.1 Economics

1.1.1 Market Analysis

The greatest measure of merit for the design of a commercial aircraft is associated with obtaining the highest possible return on investment for the airline while maintaining a safe means of transporting passengers. To accomplish this, aircraft utilization must be maximized and aircraft capacity must match passenger traffic.

The first task in defining the mission was to identify the Aeroworld market which would lead to maximum aircraft utilization. This condition occurs for long range flights which characterize the overseas market. Competition in this market will come from ships which have a higher average ticket price than trains. In the overseas market, airfares can be priced higher than in short intercontinental markets because of the higher fares charged by competitors.

The average passenger weighted distance in the targeted overseas market is 4090 ft. In the event of an emergency, an aircraft must be able to fly to the next closest airport to its original destination and loiter for 1 minute Aeroworld time. With these factors in mind, the minimum range requirement to serve the majority of the overseas market was found to be 5500 ft (includes loiter).

In Aeroworld, daily passenger traffic is assumed to be constant. The majority of routes in the long range overseas market had daily traffic figures which were evenly divisible by 40, 50 or 100. (Note: See Appendix A for a complete listing of the Request for Proposals and all given Aeroworld data.) By selecting a capacity which was evenly divisible into traffic on most routes, all passengers in the targeted market could be served with a minimum of empty seats. An aircraft capacity of 40 passengers was selected because capacities of 50 or 100 passengers would result in an

aircraft too large to meet the physical constraints of the project. A major consideration was the requirement that the aircraft be disassembled and stored in a 2 ft × 3 ft × 5 ft box (see requirements in Appendix A).

A proposed system map is shown in Figure 1-1. Solid lines represent the highest profit per hour of utilization and dashed represent the second highest profit per hour utilization. This differentiation will allow for a development of the airline in stages. For the fully developed system, there are 27 routes with 316 flights per day.
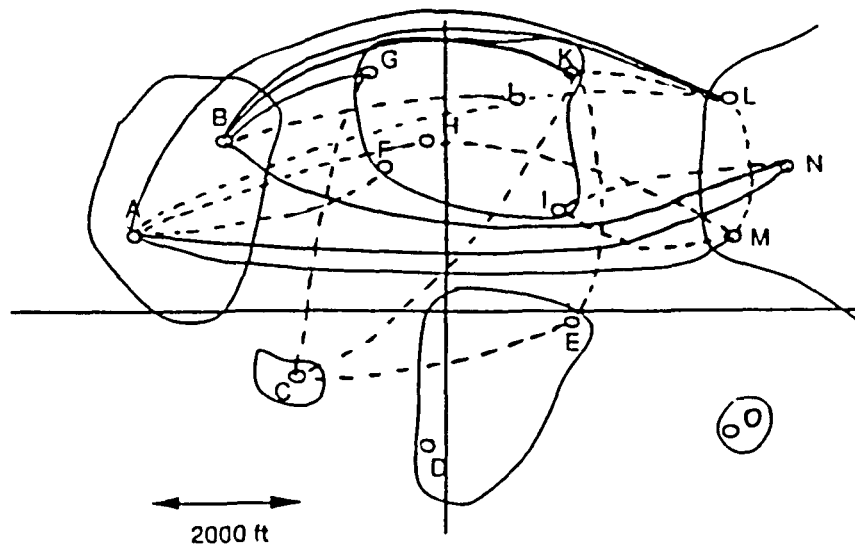
Figure 1-1. Proposed Aeroworld airline system map

1.1.2 Profitability and Investment Analysis

After identifying a market, a profitability analysis of the proposed system was undertaken. Profit was defined as revenue minus expenses where revenue and expenses were calculated as follows:

Revenue = # passengers *(flat rate fare + rate/ft *distance)

Expenses = fixed expenses + distance *(fuel/ft)

$$\text{Fixed expenses} = \text{Maintenance} + \left(\frac{\text{production cost}}{\text{\# flights/life}}\right) + \text{Takeoff fuel}$$

Labor costs for flight crews and support personnel were not incorporated into the analysis at this time. Fuel costs were determined to be the overriding expense and thus the driving concern. Maintenance and production costs were included in the above definitions because they had the potential to be effected in the design of the *Hotbox*. Labor costs will be considered later in this section.

The production cost of the *Hotbox* has a maximum value of $152,000. This number is based on the maximum number of man-hours that team members have available to devote to construction (640 man-hours) and the limit of $225 real world dollars for materials imposed by the RFP. At a cost of $100 Aeroworld dollars per man-hour and $400 Aeroworld dollars per Real world dollars, this leads to the estimated production cost of $152,000. The aircraft will sell for $200,000.

A ticket price was set 10% above the expenses associated with fuel and the maintenance charges for battery servicing. Fuel costs were assumed to be at their highest value of $120 per milli-amp hour (see Appendix A). This led to a maximum ticket price of $38 flat rate and 9.70 per 50 feet. This was based on the passenger weighted average distance of 4090 ft. This definition of profit and ticket pricing makes ticket prices very sensitive to changes in fuel costs and to fuel efficiency.

A goal in the design of the *Hotbox* was to be competitive with train and ship fares. Figure 1-2 illustrates a comparison of ship, train, and plane ticket costs v. distance. The primary competition for the *Hotbox* comes from ship travel. At the passenger weighted average distance in the overseas market (4090 ft), a plane ticket is approximately 15% above the cost of a ship ticket. Recalling that this was based on a maximum charge for fuel and would be the maximum airfare charged, the *Hotbox* should compete well against ship travel. The added speed and convenience of air travel can reasonably account for a 15% increase in ticket cost.

Ticket Costs v. Distance
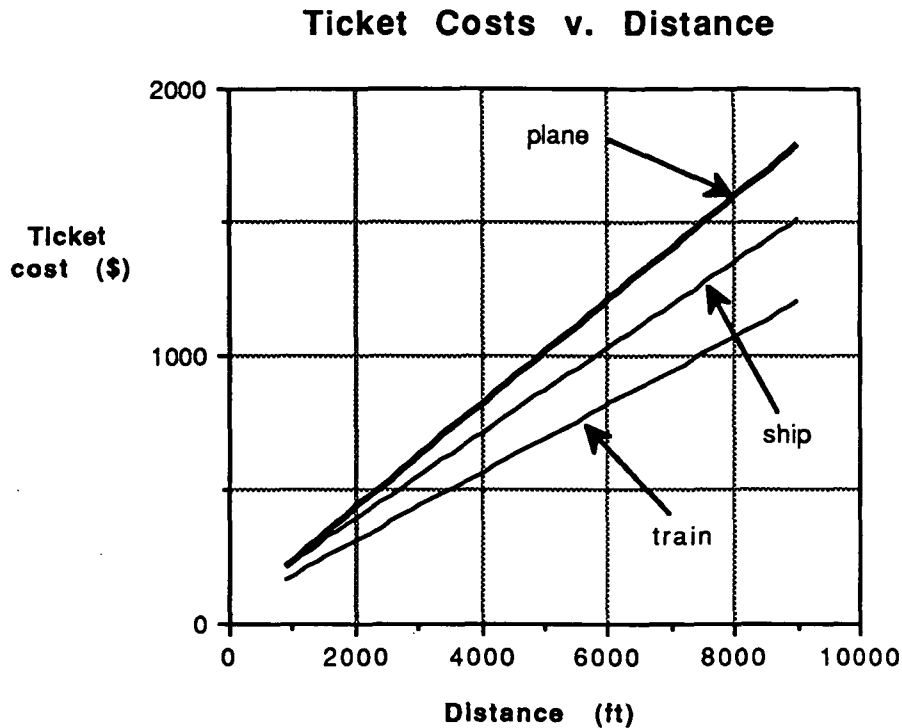
Figure 1-2: Ticket prices v. distance for modes of transportation in Aeroworld

For the system proposed earlier, a passenger load of 4.6 million passengers annually was estimated. Along with the proposed ticket cost, this leads to an operating revenue of over $3.8 billion.

To estimate previously undefined expenses, a book (Reference [1]) by George James entitled *Airline Economics* was consulted. First, the personnel needed to run the proposed airline and their salaries were estimated in order to generate a labor cost. According to industry data found in James' book, Aeroworld fuel costs were not proportional to Real world costs. Consequently, we set our other expenses proportional to our Labor costs. Table 1-1 illustrates a partial income statement for the airline with the estimated revenue and expense values. These estimates led to operating expenses of just over $3.7 billion. And an Operating Profit of $132.7 million. Based on general accounting standards, General and Administrative costs

are typically 1/3 of total expenses for a business. General and Administrative expenses were estimated to be 1/3 of expenses excluding fuel costs. This led to a Net Income estimate of $42.3 million.

Estimated Airline Income Statement
For the period of one year
(Millions of Dollars)

Operating Revenue		$3879.4
Operating Expense		
Fuel	$3254.4	
Maintenance	250.8	
Labor	98.0	
Commissions	12.4	
Passenger Food	8.4	
Landing Fees	4.8	
Advertising & Promotion	4.0	
Depreciation	70.7	
Other	43.2	
Total Operating Expense		3746.7
Operating Profit		$ 132.7
General and Administrative Expense		90.4
NET INCOME		**$ 42.3**

Table 1-1: Partial income statement for Aeroworld airline.

Forty aircraft are required to make the indicated 316 flights per day. Estimating a 300 flight life per aircraft, a total fleet replacement is required 9.5 times annually. At a cost of $200,000 per plane, this leads to an aircraft investment of $68.4 million. This aircraft life expectancy was estimated based on expected material strengths. However, no standardized method for determining aircraft life was available. Thus, there is limited confidence in this estimation. Data from Reference [1] suggests an investment in ground equipment to service aircraft to be 15% of aircraft investment. This leads to a ground equipment investment of approximately $10.3 million and a total investment of $78.7 million.

These estimates lead to a Profit Margin on Sales of 1.1% and a Return on Investment of 53.8%. This Profit Margin is in line with industry standards, according to James. Return on investment is exceptionally high as a result of the disproportionately high cost of fuel in Aeroworld and the dependance of ticket prices on this fuel cost.

1.1.3 Influencing Factors

The controlling influences on the design of the aircraft from an economic standpoint center around fuel cost. Fuel expenses make up approximately 86.9% of the total operating expenses. Production costs and battery maintenance charges influenced some aspects of the design on a secondary level. Maintaining a competitive stance with respect to ship travel was also a key economic concern. But, even assuming the highest given fuel cost, plane tickets are still comparable to ship tickets. Thus, from an economic standpoint, optimizing cruise fuel economy should supersede all other economic concerns.

Aircraft cost	$152,000
Aircraft sales price	$200,000
Ticket cost	$38 + 9.70/50 ft
Net Income	$42.3 million
Total Investment	$78.7 million
Percent profit on sales	1.1%
Return on Investment	53.8%

Table 1-2: Key Economic Statistics

1.2 Mission Parameters

A maximum velocity constraint of 35 ft/sec exists in Aeroworld. A cruise velocity of 30 ft/sec was initially targeted. This velocity would allow for acceleration in banked turns to maintain a constant lift force in the vertical direction and thus a constant altitude. A cruise velocity of 30 ft/sec would also allow the pilot to increase velocity 16.7% in an emergency maneuver while still moving passengers to their destination at the fastest practical speed.

Maximum return on investment for an airline will also be achieved by minimizing investment and costs. Thus, the aircraft design must incorporate a design with minimum production cost and maximum fuel and maintenance efficiency.

After examining the request for proposals and the Aeroworld markets, Theta Group has defined its mission as follows: the construction of a 40 passenger aircraft with a minimum range of 5500 ft, a cruise velocity of 30 ft/sec, and a design which minimizes production costs and maximizes operational efficiency.

Passenger capacity	40 passengers
Cruise Velocity	30 ft/sec
Minimum Range	5500 ft
Other goals	Minimize costs Maximize return on investment

Table 1.3: Mission Definition Summary

The Mission Definition was driven by the goal of generating the highest possible rate of return on investment for the airline. This led directly to the identification of the overseas market as a target market. Passenger capacity and minimum range were established based on the requirements of profitably serving

this market. Passenger capacity was also influenced by the storage constraints imposed on the technology demonstrator. Cruise velocity was determined considering passenger convenience and safety factors, noting the maximum allowable velocity of 35 ft/sec.

1.3 Design requirements and objectives

In order to achieve the minimum goals set forth in the Request for Proposals and in the Mission Definition, several additional requirements where placed on the design. The requirements were imposed in the following areas:

Airframe Structure and Materials

- Total technology demonstrator takeoff weight will not exceed 4.5 lbs (72 oz). Data from the construction of previous RPV's indicated that minimizing weight greatly improved the probability of a successful flight. Based on this prior data and estimates of the necessary component weights of a commercial transport, a maximum weight of 4.5 lbs established.

- The structure must meet the requirements for utilizing a 5 ft gate. The airports in the Aeroworld market targeted are dominated by 5 ft gates. In order to have the maximum number flights per day, the design must be able to utilize a 5 ft gate.

- The aircraft will carry 40 passengers and a 3 member flight crew in a single class seating arrangement. This capacity meets the requirements of the Mission Definition. Single class seating is common on smaller aircraft and it provides for greater simplicity in construction and in ticket pricing.

- The design must allow for a battery pack exchange within 1 minute in order to minimize battery maintenance charges.

- The complete aircraft must be able to be disassembled for transportation and storage and fit within a storage container no larger than 2x3x5 ft. This is a requirement imposed by the Request for Proposals.

Propulsion System

- A single electric powered engine will be used. A single engine design reduces weight and makes the RPV easier for a pilot to fly.

Flight Control System

- Aircraft control surfaces will include a rudder and an elevator operated by 2 S28 servos. This will minimize aircraft equipment weight. It also leads to greater simplicity in the aircraft design.

- The radio control system and instrumentation package must be removeable and a complete system installation must be accomplished within 30 minutes. This is stipulated in the Request for Proposals.

Performance

- The aircraft must have a range of at least 5500 ft and cruise at a velocity of 30 ft/sec, as outlined in the Mission Definition.

- Takeoff must be accomplished within 60 ft. This will allow service to all airports in the previously defined market and to nearly all cities in Aeroworld.

- The aircraft must be able to achieve a 60 ft. radius level turn

Economics

- Production will be accomplished in a maximum of 640 man-hours. This will minimize labor costs.

- Material costs will not exceed $220 real world dollars, excluding the instrumentation and propulsion systems. Again, this will minimize production costs.

1.4 Concept Selection

In arriving at the final design concept, a number of concepts were considered. Among these were a flying wing design, a swept wing design, and the rectangular wing design. Among the considerations were the ease of construction, the availability of data from similar aircraft which have been built previously, the number of engineering difficulties which were foreseen, and the amount of work which could be accomplished within the limited seven week design schedule.

1.4.1 Flying Wing

The first concept considered was a flying wing design illustrated in Figure 1-2. This design offered several unique advantages over conventional aircraft. Preliminary estimates indicated that a passenger capacity of 100 ping-pong balls could be achieved in an aircraft which met all size and weight requirements. The absence of a fuselage would lead to a decrease in drag and a decrease in the power required to fly the aircraft.

However, many problems were foreseen with the flying wing. First, a propeller located at the leading edge of the airfoil would disturb the airflow over a great deal of the wing. Thus, a pusher propeller was suggested. Since the airfoil tapers down at the trailing edge, the motor would have to be located far enough from the trailing edge to provide adequate structural integrity for the mount the motor. This leads to the need for a very long propeller shaft. The rotational motion of the shaft and the vibrations produced by the engine were predicted to produce significant displacements at the propeller.

With the propulsion system located in the aft of the aircraft, a large portion of weight would be required near the leading edge to yield an aircraft center of gravity suitable for aircraft stability and control. Very little space exists forward of the passenger compartment to position the battery pack and the instrumentation

FLYING WING

14"

26.5"

28.75"

12"

27.2"

3.9"

1.7'

84"
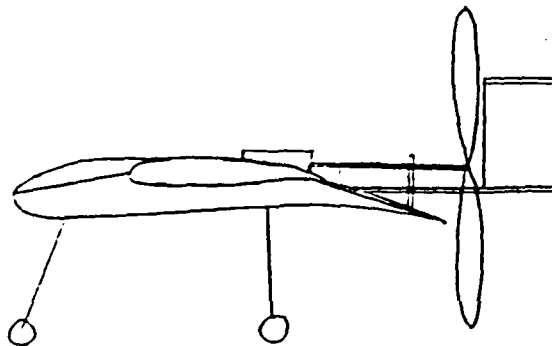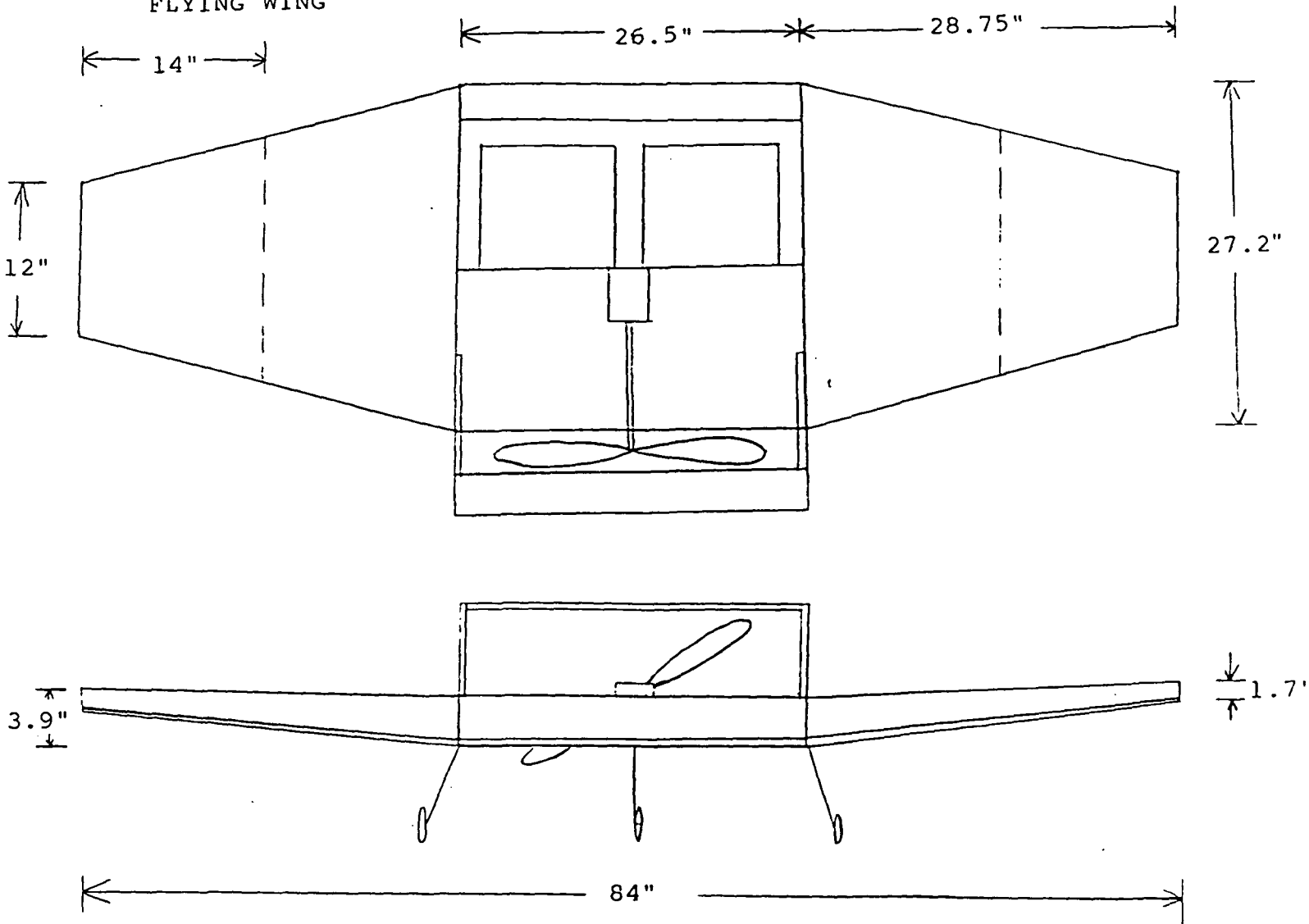
SWEPT WING
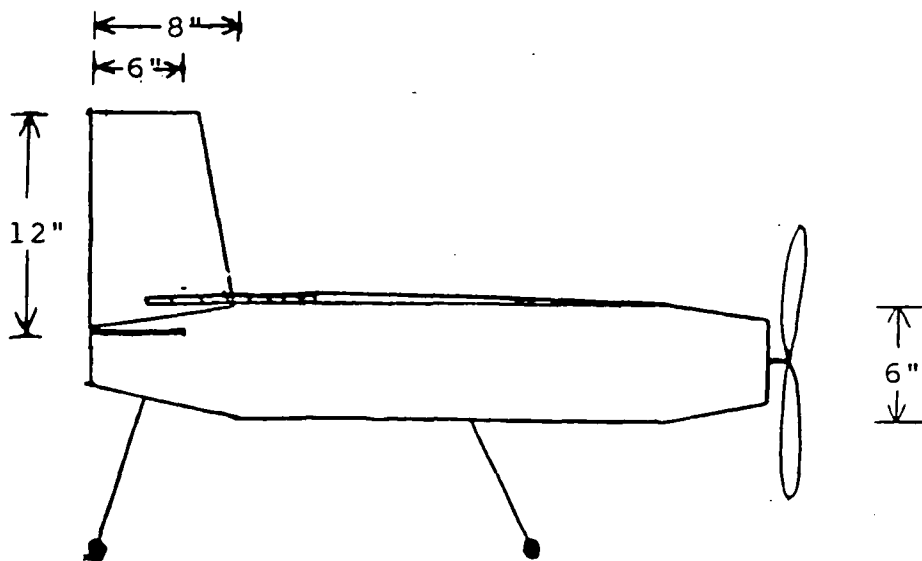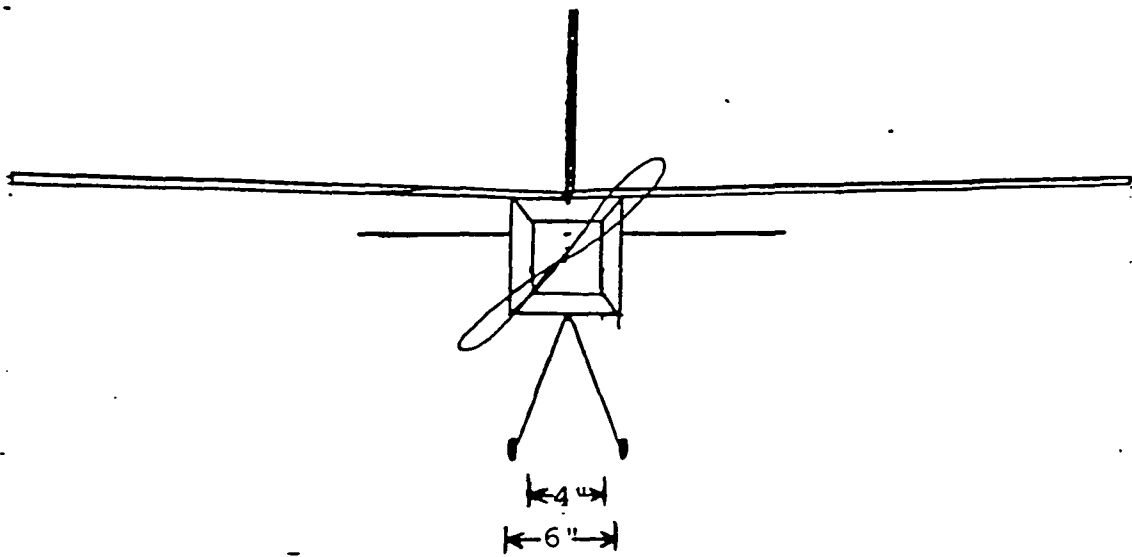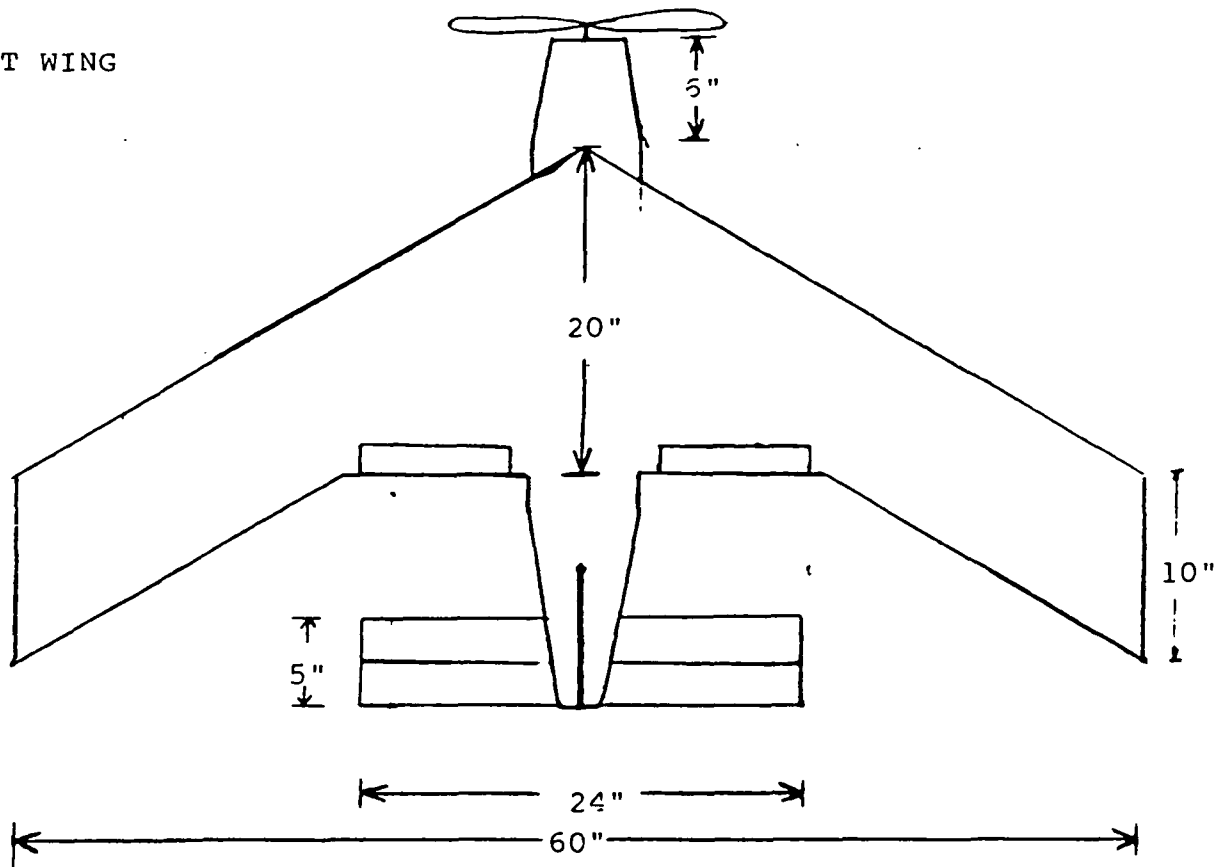
package. The feasibility of locating all this equipment in an accessible location without severely disrupting the leading edge of the airfoil was a significant technical challenge.

Considering the short seven week design period allotted for concept development, the technical problems of the flying wing design were judged to be to great.

1.4.2 Swept Wing

The swept wing design, shown in Figure 1-3, illustrates a more conventional design with several significant advantages. The five foot wing span would enable it to fit into the five foot gates of Aeroworld without the need for folding wings. Also, the design had a the benefits of reduced induced drag available from a high aspect ratio (AR≈7.0) construction.

However, this concept also had some undesirable qualities. First, the varying chord associated with this planform would make construction difficult and very time consuming. This would significantly increase production costs. Second, this aircraft incorporated a two level seating arrangement with a third level required for gear. Because of this three level configuration, the frontal area would be extremely large leading to drag penalties. Packing everything into three levels also led to a shorter fuselage and a decreased empennage moment arm. This was seen as a potential source of poor stability and control.

1.4.3 The *Hotbox*

The final design concept, called the *Hotbox* , is illustrated in Figure 1-4. The *Hotbox* has a wing of rectangular with no taper or sweep. This design leads to ease of construction and thus smaller production costs. Data from past RPV's indicated

The Hotbox
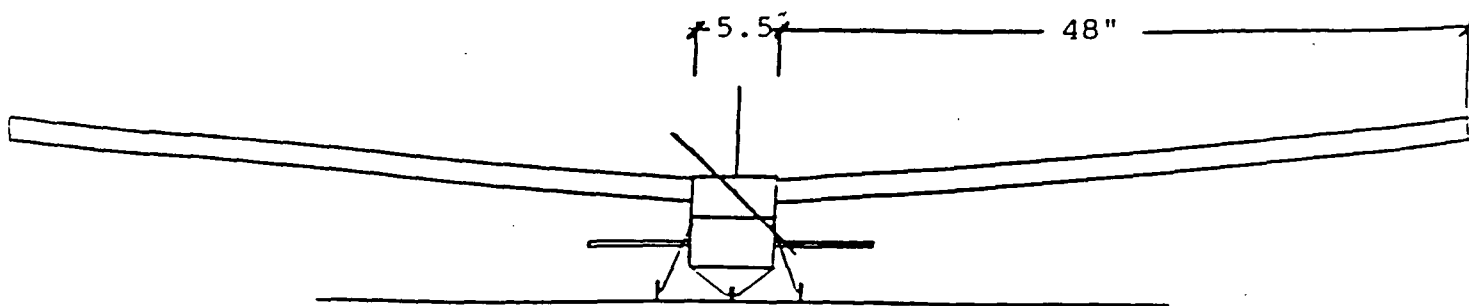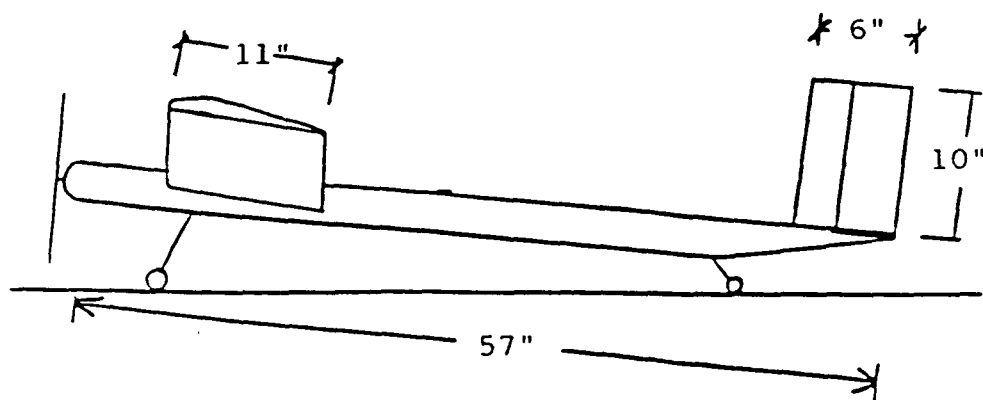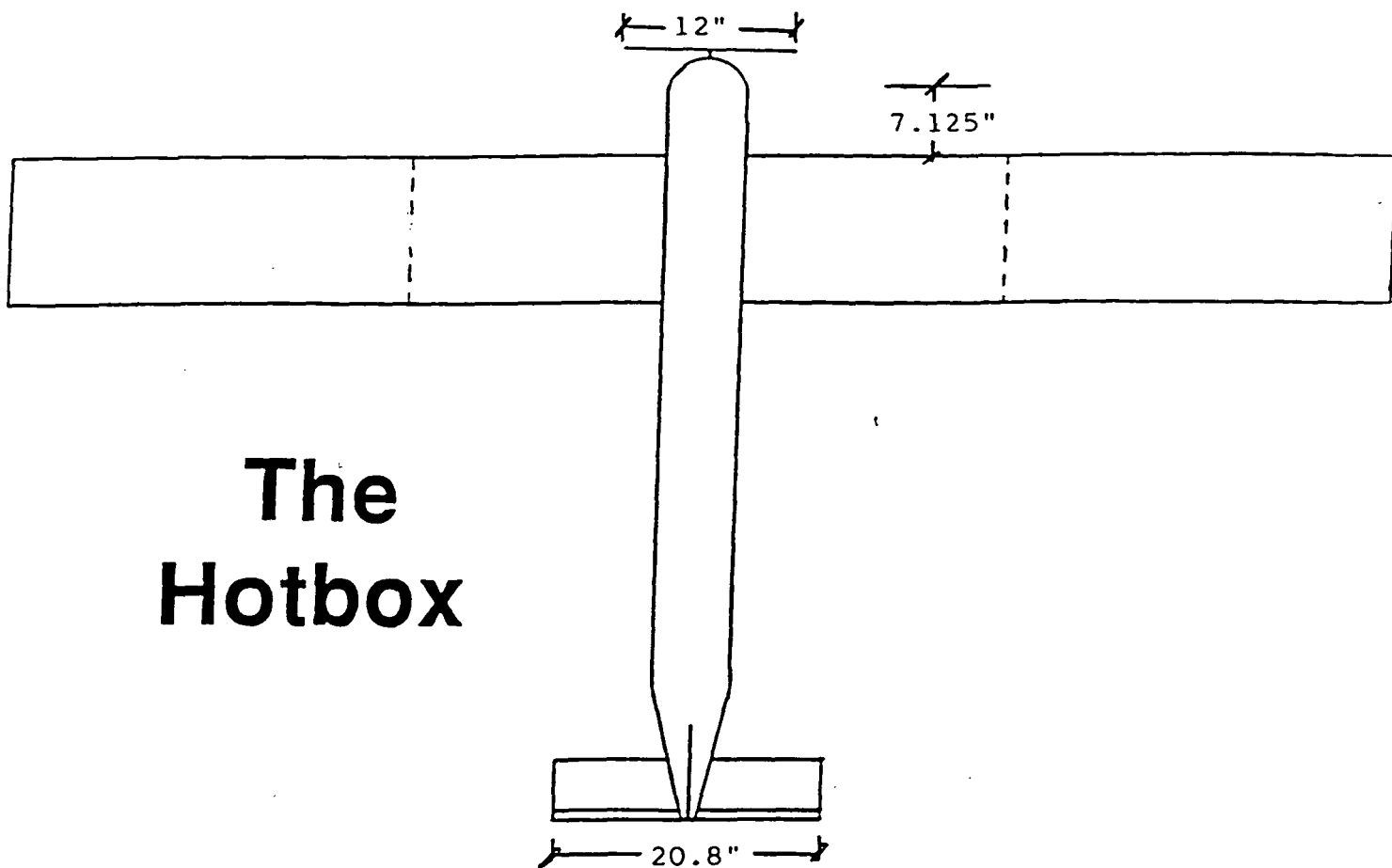
that an aspect ratio on the order of 8-10 and a wing loading between 9-11 oz/ft^2 were desired. In order to achieve these values, a span longer than 5 ft was needed. Thus the *Hotbox* incorporates a hinged wing design.

A 2x20 seating arrangement was incorporated into the design to reduce frontal area and to extend the empennage moment arm. A six inch area was inserted between the passenger compartment and the motor for placement of the battery packs, servos, speed controller, receiver, and the through beam of the wing. Positioning this gear forward of the quarter chord helps to position the center of gravity at the 30 percent chord location with the aircraft filled to capacity. The center of gravity will move forward as passengers are removed.

The internal configuration of the *Hotbox* is shown in Figure 1.5. The crew contains a pilot, copilot and flight attendant. In the technology demonstrator, the pilot and copilot are replaced by the radio gear. The flight attendant's fold down seat is located next to the door which is across from the galley. The *Hotbox* contains single-class 2x20 seating.

1.4.4 Influencing Factors

The selection of the *Hotbox* concept was strongly influenced by the constraint of the seven week design period. Non-conventional designs were ruled out because the seven week design period was believed to be too short to overcome all of the technical challenges associated with a radical design.

Construction considerations also significantly influenced the development of the *Hotbox* concept. Ease of manufacturing was seen to be an efficient means of cutting cost and reducing errors. As expected, all of the requirements imposed by the request for proposals, the mission definition, and the design requirements and objectives played a significant role in concept development.
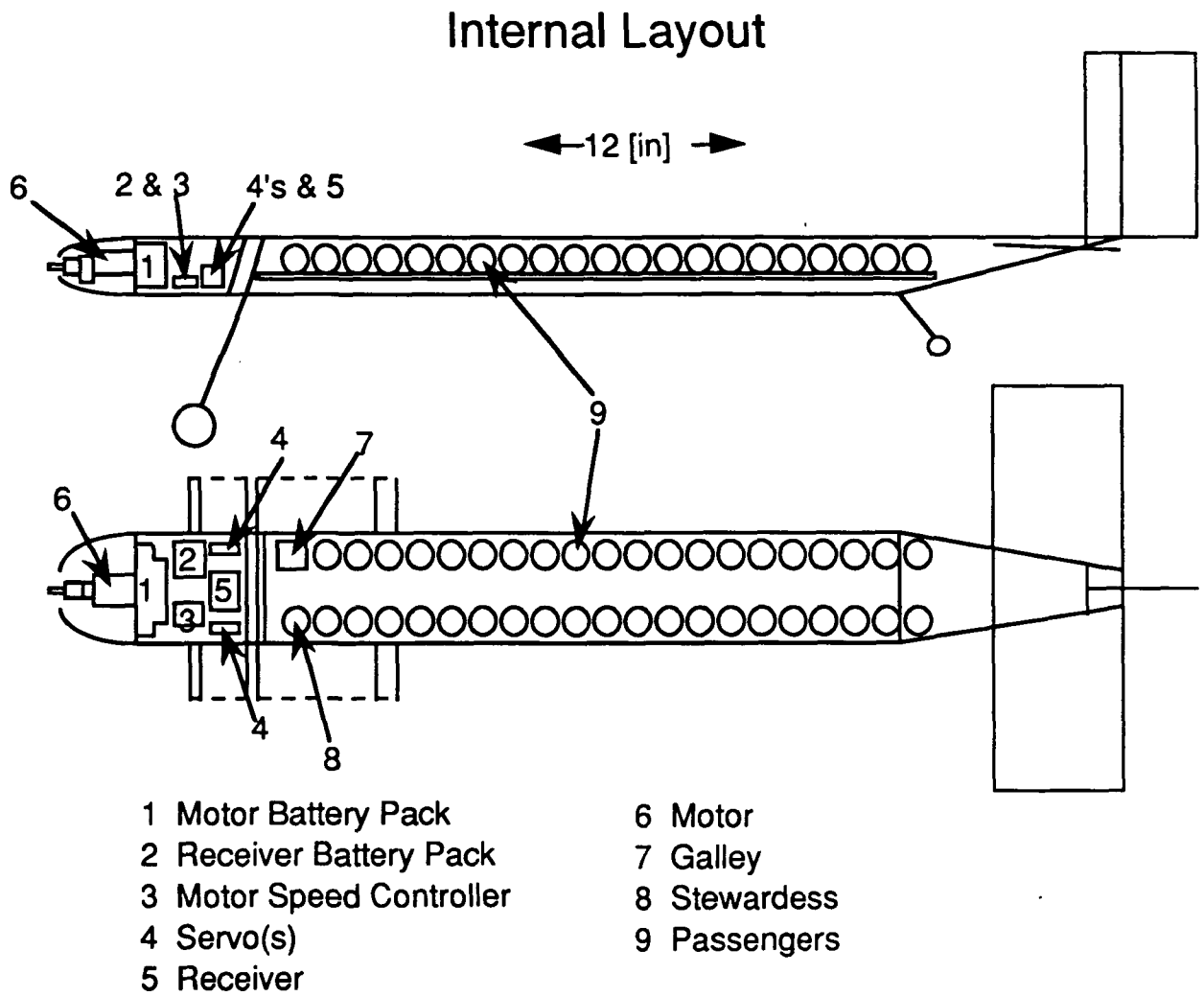
Internal Layout

1 Motor Battery Pack   6 Motor
2 Receiver Battery Pack   7 Galley
3 Motor Speed Controller   8 Stewardess
4 Servo(s)   9 Passengers
5 Receiver

Figure 1-5: Internal configuration.

2. AERODYNAMICS

2.1 System Requirements

The chief goals of the aerodynamics group were to:

- Provide sufficient lift during takeoff, landing, and cruise
- Minimize aircraft drag
- Include cost effectiveness in design choices.

2.2 Airfoil Selection

The selection of the airfoil was a crucial part of the airplane design. Since the *Hotbox* will operate in a low Reynold's number regime (Re = 1×10^5 - 3×10^5), only those airfoils which perform well at low Reynold's numbers were considered. In order that the proper airfoil could be chosen, a list of criteria based on C_{lmax}, stall angle, lift curve slope, and shape of the airfoil was chosen.

Sketches and lift curve data from Reference [2] were examined. On the basis of the above criteria, the many airfoils were narrowed down to three airfoils. Each of these three airfoils were selected on their individual merits which are listed in Table 2.1 below.

Airfoil	Positive Characteristics
Spica	High α_{stall}, feasibility in construction
Wortmann FX-63-137	High lift curve data
S3010	Low C_{do}, high lift to drag ratio

Table 2.1 Initial Airfoils and their Characteristics

Takeoff and cruise requirements made it necessary to set minimums on C_{lmax} and stall angle for our airfoil. The minimum lift coefficient was set at 1.0 and the stall angle of the airfoil could not be less than $10°$. These

constraints were sufficient to allow for margins of safety especially during takeoff. Figure 2.1 shows the infinite lift curves (without stall regions) for the above airfoil sections.

Comparison Lift Curve Slopes
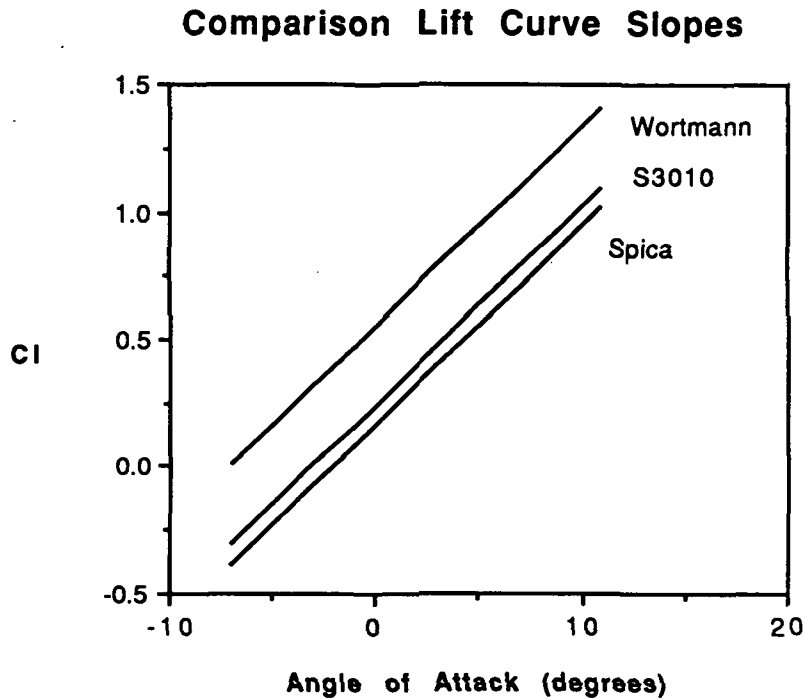
Figure 2.1 Infinite Lift Curve Slope for 3 Airfoils

The S3010 produced the least drag and had a C_{do} of 0.012; however it stalls at a low angle of attack of 10°. Because the S3010 and the Spica were roughly similar, the S3010 was eliminated from consideration because of its low stall angle in favor of the Spica airfoil. Table 2.2 shows the two remaining airfoil sections and their characteristics.

Airfoil	C_{lmax}	α_{stall}	C_{do}	t/c
Spica	1.4	14°	0.03	11.7%
Wortmann	1.6	12°	0.033	13.6%

Table 2.2 Spica and Wortmann Airfoil Characteristics

The chief factors in the final decision to pick the Spica airfoil rested primarily with economic and structural reasons. The Spica airfoil was chosen based on its feasibility of construction. Because it is a flat-bottomed airfoil, it will be easier to machine , consequently easier and quicker to produce, thus driving down production costs. The Spica airfoil from a structural standpoint is better for attaching monokote than the Wortmann airfoil. As shown in Figure 2.2, the Wortmann airfoil has a concave trailing edge.

FX63-137
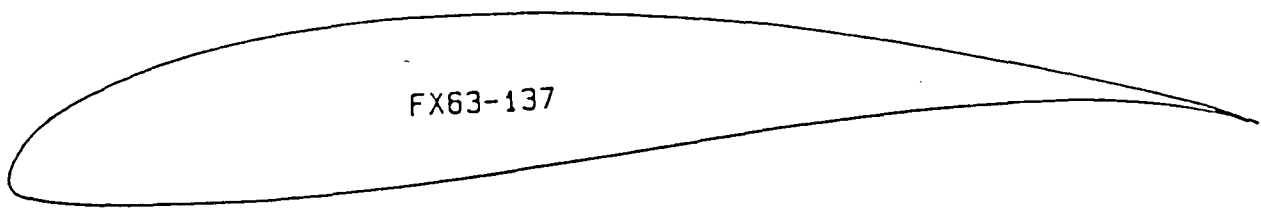
Figure 2.2 Wortmann Airfoil
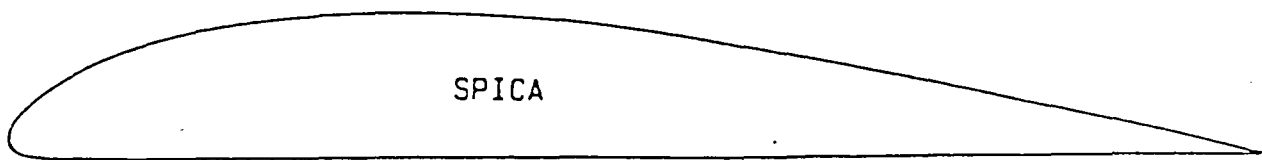
SPICA

Figure 2.3 Spica Airfoil

- thickness = 11.7 %
- α_{stall} = 14 °
- $\alpha_{L=0}$ = -2.0 °
- camber = 4.75 %
- C_{lmax} = 1.4

When the monokote is attached to this airfoil, it is not guaranteed to adhere closely to the shape near the trailing edge. On the other hand, the Spica airfoil will allow the monokote to be attached easily and will not undergo deformation of the airfoil shape. Figure 2.3 shows the Spica airfoil along with its various characteristics.

2.3 Wing Design

Initially wing design began by looking at the aircraft loading. In Figure 2.4, wing loading is plotted versus weight for wings of different areas.

Wing Loading vs. Weight (Varying Area)
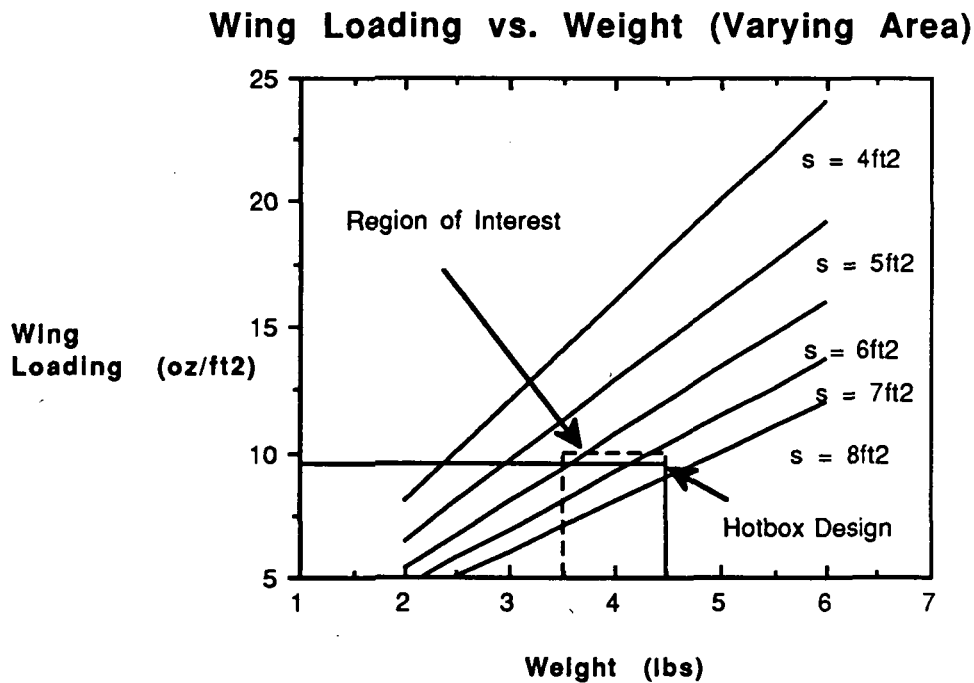
Figure 2.4 Plot of Wing Loading

From the database, it was recommended that a wing loading between 9 and 11 oz/ft^2 was desirable. Our initial weight estimate was for 3.5 lbs and our

maximum weight was targeted at 4.5 lbs. This area is blocked out in Figure 2.4, and as can be seen, only wing areas of 6, 7 or 8 ft^2 meet these requirements.

The next parameter to be varied in this study was the area and aspect ratio as a function of the chord length. These two parameters are plotted in Figures 2.5 and 2.6 respectively.

Area vs. Chord Length
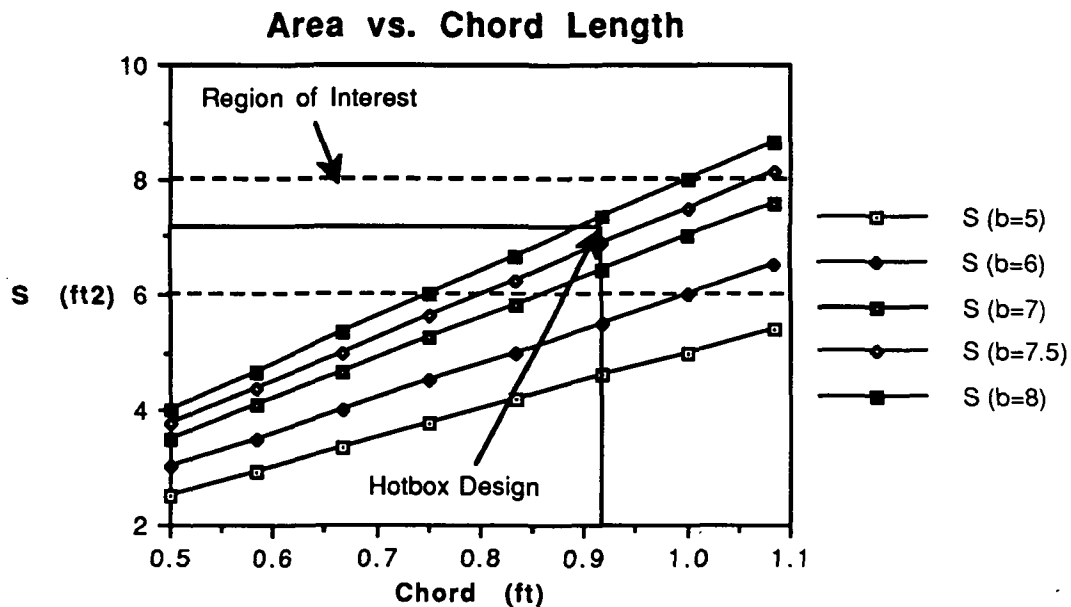
Figure 2.5 Wing Area as a function of chord length

In figure 2.5, the target areas are blocked off. Chord lengths are plotted for spans of varying length. From the graph, it can be seen that only spans of 6-8 feet can accommodate the area requirement set by wing loading. In Figure 2.6, aspect ratio is plotted against chord length for several different spans. The plot shows the decrease in aspect ratio with increasing chord length for a fixed span length.

Aspect Ratio vs Chord (Varying Span)
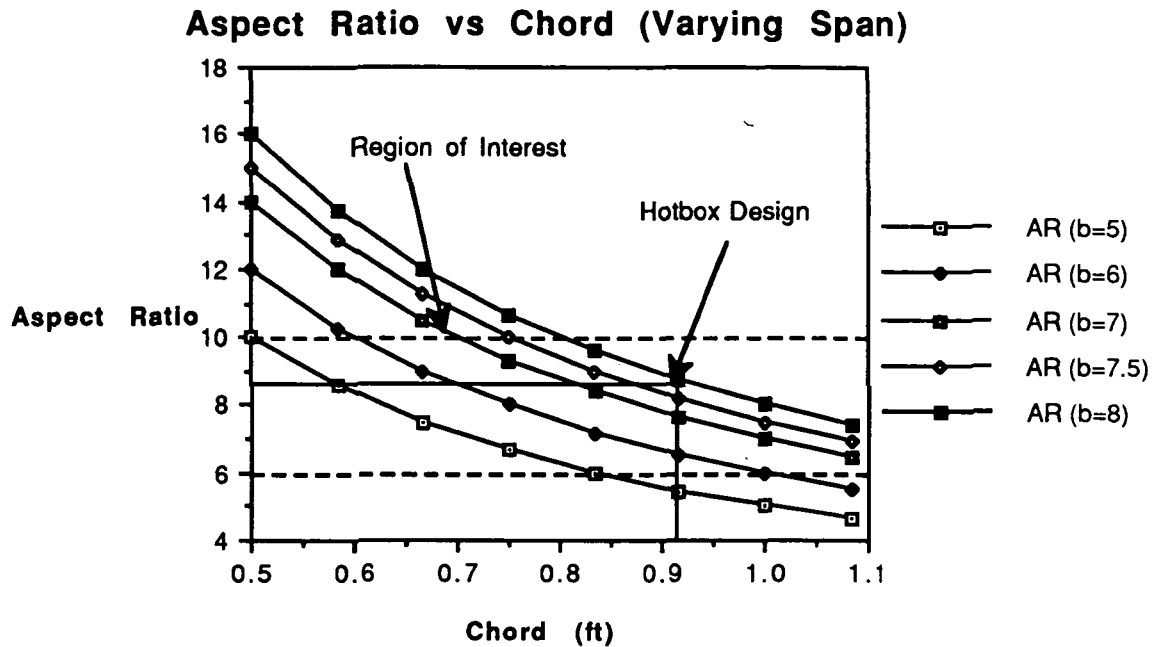
Figure 2.6 Aspect Ratio as a function of Chord Length

To examine the effect of aspect ratio on the lift coefficient of the airfoil, the lift curve slope of the Spica airfoil up to 10° was plotted for the infinite case, and varying aspect ratios. It is shown in Figure 2.7. The lift curve of the infinite case was corrected using the equation:

$$a = \frac{a_O}{\left[1 + \frac{a_O}{(\pi\ AR\ e)} \right]}$$

As can be seen from the graph, the lift curve severely degenerates for the low aspect ratio of 4 and does not even meet the minimum C_{lmax} requirement. As the aspect ratio increases, the curves move closer to the infinite line. The curves for aspect ratios of 8 and 10 are starting to fall on top of one another. Taking note of this behavior, the aspect ratio range for the wing was set between 6 and 10 which would not decrease the lift curve slope significantly. This range of aspect ratios has been blocked out in Figure 2.6

Lift Curve Slope Spica (Different AR)
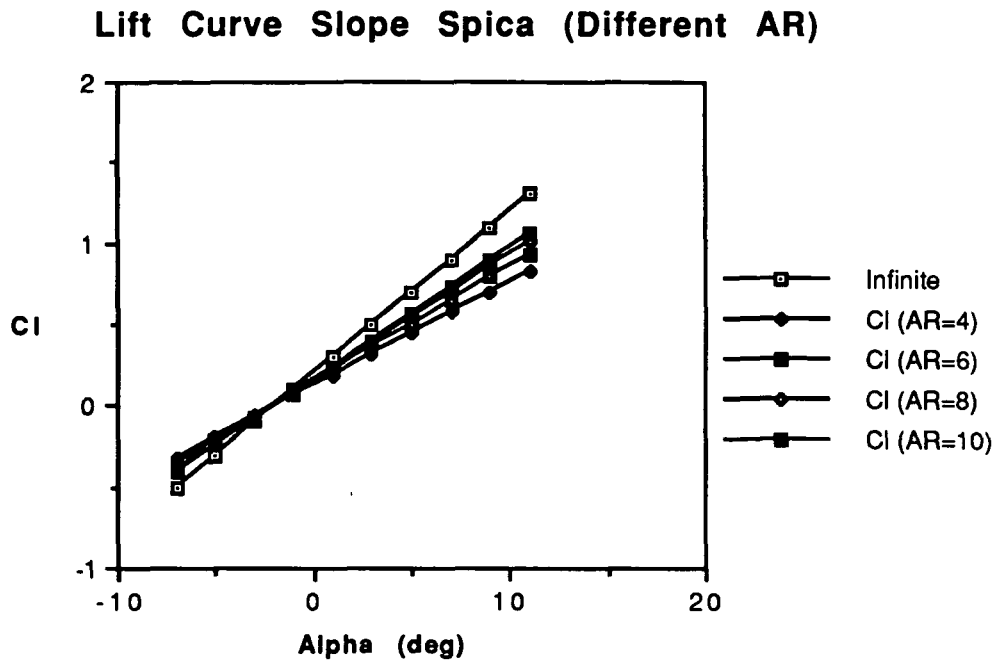
Figure 2.7 Lift Curve Slopes for the Spica Airfoil

The wing will not be tapered, twisted or swept. The positive effects of taper, such as increased lift and reduced drag, were outweighed by the feasibility in constructing a rectangular wing. Twist was not added because of the additional construction difficulties. Because the aircraft will operate in negligible Mach ranges, sweep was not considered.

The final design of the wing was set at an area of 7.33 ft^2, a chord of 11 inches, and an aspect ratio of 8.72. Dihedral was required for turning. The amount of dihedral was determined by control analysis and will appear later in the report in the stability and control section. Further analysis later in the project indicated that the benefits of choosing this size wing were reduced drag coefficient and decreased power required. As a final note, had our initial weight estimate been met, more emphasis would have been placed on other benefits or disadvantages of picking the aspect ratio. Table 2.3 lists the final design parameters for our wing. Also shown is Figure 2.8, the lift curve for

the Spica airfoil which was corrected for an aspect ratio of 8.72. (Note that the stall region was an estimate because the corrected lift curve was based only on the constant slope portion of the infinite lift curve data.)

Planform area, S	7.33 ft^2
Aspect Ratio, AR	8.72
Wing Span, b	8.0 ft
Mean Chord, c	11.0 inches
Airfoil Section	Spica
Taper Ratio	1
Twist	none
Sweep	none
Incidence Angle	5°
Dihedral	7°
Cruise C_L	0.57

Table 2.3 Final Wing Characteristics

Lift Curve of Spica Airfoil (AR=8.72)
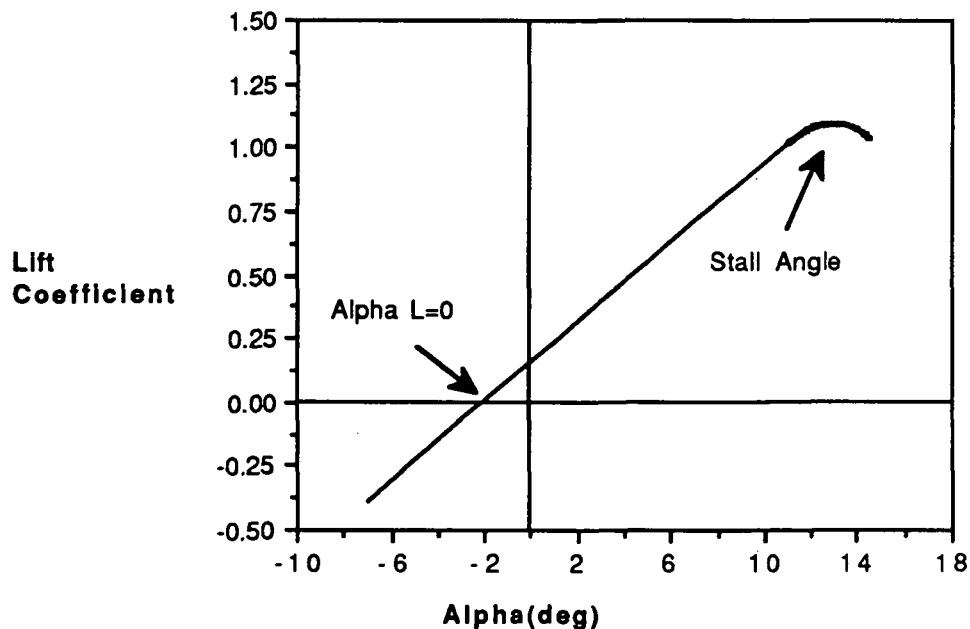
Figure 2.8 Lift Curve for the Spica Airfoil (AR=8.72)

2.4 Drag

Drag is an important parameter affecting the design and performance of an aircraft. The drag acting on an aircraft directly dictates the power required for flight, and therefore greatly influences the selection of the engine, power source, and the propeller. The power required is also directly related to the range and endurance of the plane, both of which are crucial to the profitability of a commercial transport. The importance of drag makes it desirable to reduce drag when feasible, and to continually provide accurate estimates of the drag during the design process.

2.4.1 Drag Prediction

To predict the total drag on the *Hotbox*, it was necessary to estimate both the parasite drag, $C_{d,0}$, and the efficiency factor, e, for the aircraft. With these quantities and the aspect ratio of the wing known, a 2-parameter drag polar could be made of the form

$$C_D = C_{D,0} + \frac{C_L^2}{\pi e AR}$$

Parasite drag estimates were made using two different methods. The first was an empirically determined formula that estimated drag based solely on the total wetted area of the aircraft. As presented in Reference [3], this formula was:

$$C_{D,0} = 0.0055 \frac{S_{wet}}{S_{ref}}$$

This method did not seem to account for drag of the landing gear, so an additional 0.0095 was added to the total. This landing gear drag was estimated from experimental data on similar landing gear, as given in Reference [4] The result of this method was a parasite drag coefficient of 0.027.

A second method used was a drag breakdown technique taken from a handout entitled *Sub-sonic Drag Breakdown Method* by Dr. R. Nelson which was distributed to Notre Dame's AERO 348 class. This method involved breaking the aircraft down into its major components and estimating the drag on each with reference to the planform area of the wing. The total parasite drag was found using the equation:

$$C_{D,0} = \frac{S\,(C_{Dp}\,A_p)}{S_{wing}}$$

Values for C_{Dp} were taken from Reference [4] and the handout. Finally, 15% was added on to the calculated parasite drag to account for roughness and interference drag, as recommended by Nelson.

Table 2.4 shows the C_{Dp}, the reference area, the contribution to the total drag, and the reference from which C_{Dp} was taken for the various aircraft components.

Component	C_{Dp}	A_π (ft2)	% of Total Drag	Reference
Fuselage	0.9	0.104	40	Hoerner 3-7 fig. 32
Front Landing Gear	0.5 per side	0.0668	30	Hoerner 13-5 fig. 35
Wing	0.007	7.33	22	Nelson p.2
Tail Landing Gear	0.2	0.0122	4	Hoerner 13-5 fig. 33
Horiz. Tail	0.008	0.55	2	Nelson p.2
Vert. Tail	0.008	0.45 .	2	Nelson p.2
Add 15% ---		Total $C_{D,0}$ =	0.034	

Table 2.4 Component Breakdown of Drag

The final $C_{D,0}$ for the aircraft was 0.034 and based on Nelson's method which seemed the most reliable based on existing data.

The efficiency was estimated by using the equation:

$$\frac{1}{e} = \frac{1}{e_{wing}} + \frac{1}{e_{fuselage}} + \frac{1}{e_{other}}$$

which was given in both References [3] and the handout. The values for e_{wing} and $e_{fuselage}$ were obtained from Figures 2.9 and 2.10, taken from Reference [3] page 94.
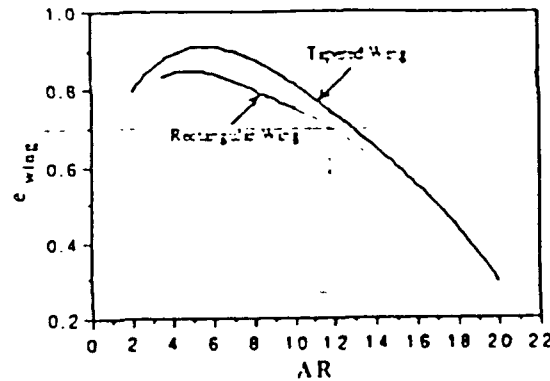
Figure 2.9: Wing Efficiency Factor
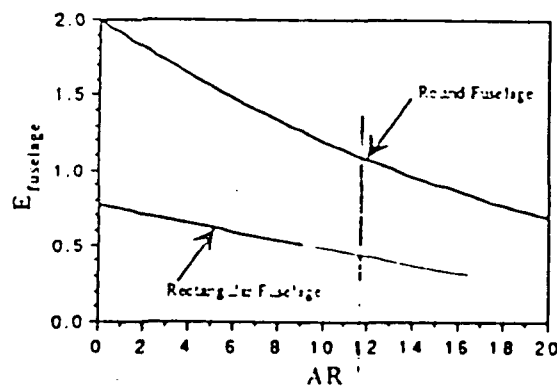
Figure 2.10: Fuselage Efficiency Parameter

The *Hotbox* has a wing aspect ratio of 8.72, from which Figure 2.9 gives e_{wing} to be about 0.78. The aspect ratio of the fuselage is 14.0 from which Figure 2.10 gives $E_{fuselage}$ to be about 0.4. Using this value and the relation

$$e_{fuselage} = \frac{(E_{fuselage})(S_{wing})}{S_{fuselage}},$$

where $S_{fuselage}$ is the maximum frontal area of the fuselage, $e_{fuselage}$ was found to be 25.5. The references recommended that e_{other} be taken to be 20. These values lead to :

$$\frac{1}{e} = \frac{1}{0.78} + \frac{1}{25.5} + \frac{1}{20}$$

$$e = 0.73$$

With the parasite drag, the efficiency, and the aspect ratio known the equation for the drag polar was found to be:

$$C_D = 0.034 + 0.050 \, C_L^2$$

A plot of this drag polar is shown in Figure 2.11.
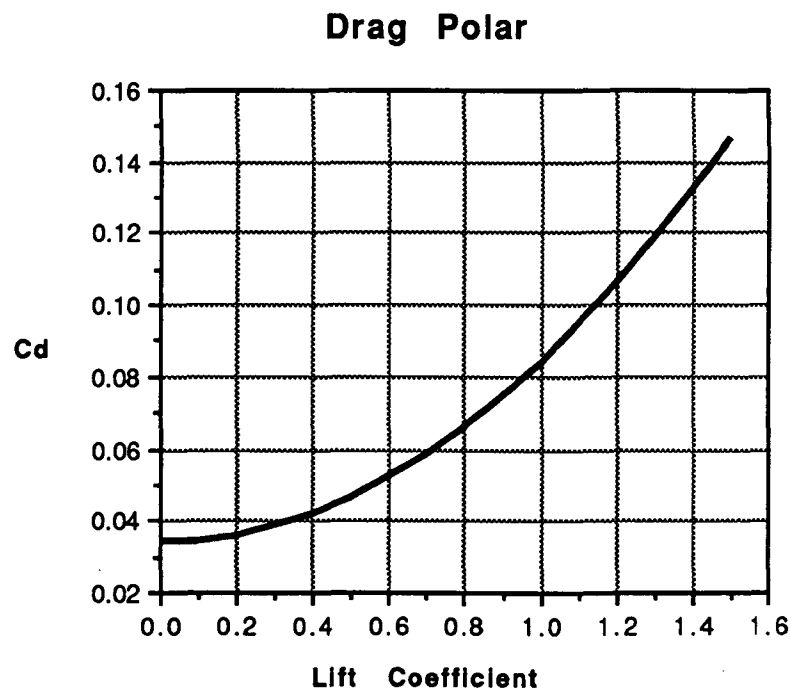
Drag Polar

Figure 2.11 Drag Polar for Aircraft

For the planned cruise velocity of 30 ft/sec, the required lift coefficient is 0.57. Using this value in the drag polar equation indicates that the parasite drag at cruise will be more than twice that of the drag due to lift. Therefore, it is the

parasite drag that should be primarily targeted in any attempt to reduce total drag.

The largest portions of the parasite drag for the *Hotbox* came from the landing gear and the fuselage. The landing gear are bluff bodies, and therefore have very high drag coefficients. In order to reduce this drag the use of fairings will be considered, although difficulty in construction may rule this out. According to Reference [4], the use of fairings could reduce the landing gear drag coefficient by 30-35%. The design of the fuselage for the *Hotbox* was most affected by the payload it was required to carry and ease of construction. There was therefore little done to reduce its drag, with the exception of minimizing the frontal area. The sensitivity of parasite drag to frontal area is illustrated in Figure 2-12, assuming all other parameters are held constant.

Parasite drag v. Frontal area
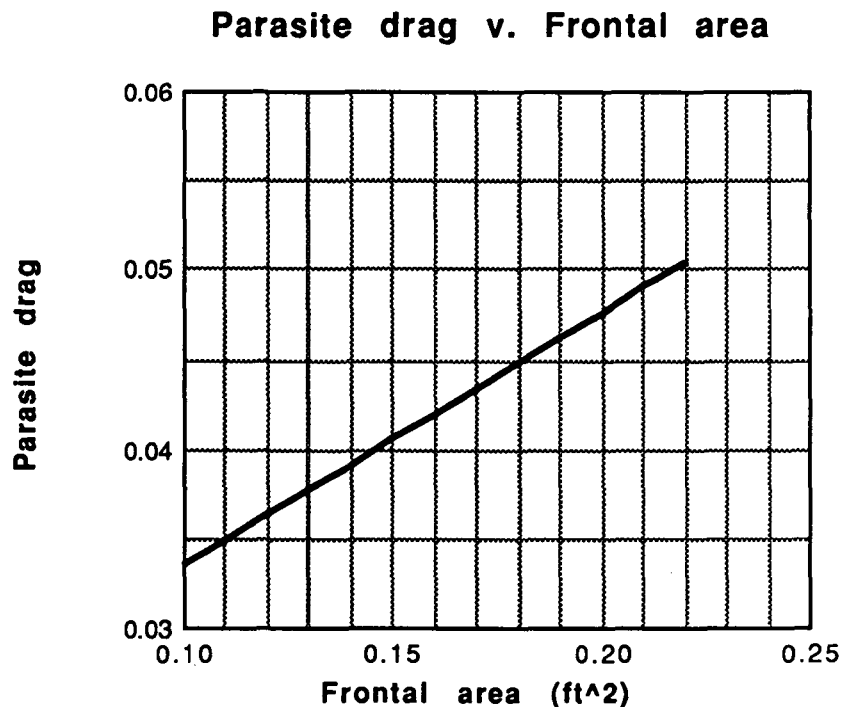
Figure 2-12 Parasite drag v. Frontal area for the *Hotbox*

2.5 Aerodynamic Estimates

A software package called LinAir was used to determine $C_{L\,max}$, the lift curve slope, α_{stall}, and $\alpha_{L=0}$ for the entire aircraft. This program used lifting line theory to estimate the interaction between the components of the aircraft, which were modeled as flat plates. The program also took into account the characteristics of the airfoil sections used for the lifting surfaces by using the coefficients resulting from a polynomial curve fit of their drag polars. Figure 2.13 shows the flat plate model to represent the *Hotbox*.
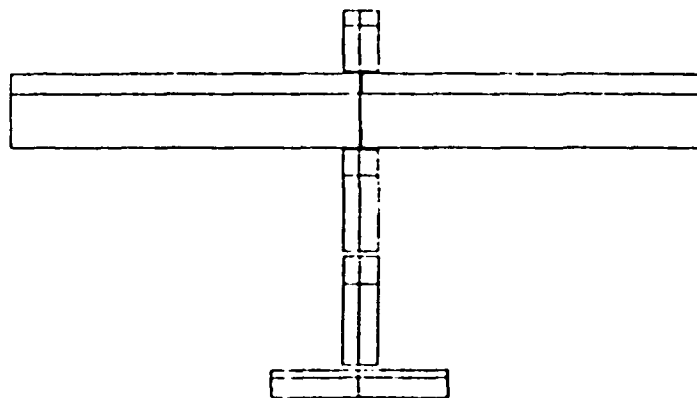
Figure 2.13 Flat Plate Model of the *Hotbox*

To calculate the stall angle of attack, the lift distributions given by LinAir were examined for various angles of attack. When the local lift coefficient at any spanwise location exceeded C_{Lmax} for the Spica airfoil, the aircraft was considered to be stalled. This first occurred at a fuselage angle of attack of 8.6°. Figure 2-14 shows the spanwise lift distribution at an aircraft angle of 8.6°. At this angle, the lift coefficient was 1.25, which was taken to be C_{Lmax} for the aircraft.

**Lift distribution over the wing span
(at aircraft angle of attack =8.6°)**
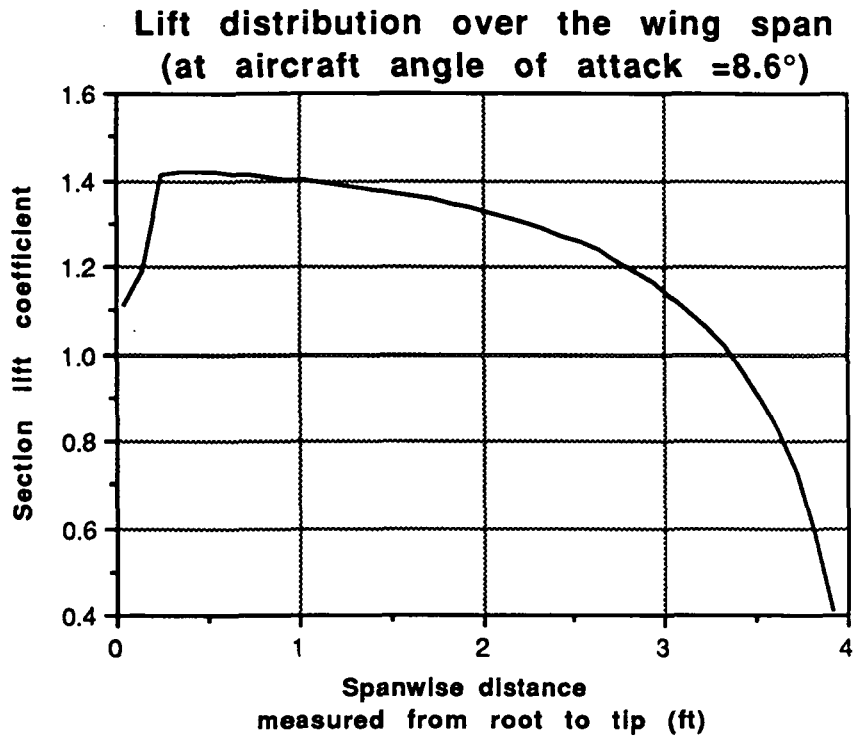
Figure 2-14 Lift distribution over the *Hotbox* wing span

The lift curve slope of 0.085 was found by plotting total C_L calculated by LinAir at various angles of attack. Using this lift-curve slope, C_{Lmax}, and α_{stall}, $\alpha_{L=0}$ was found to be -6.1° with respect to the fuselage. A plot of the *Hotbox's* lift curve is shown in Figure 2.15.
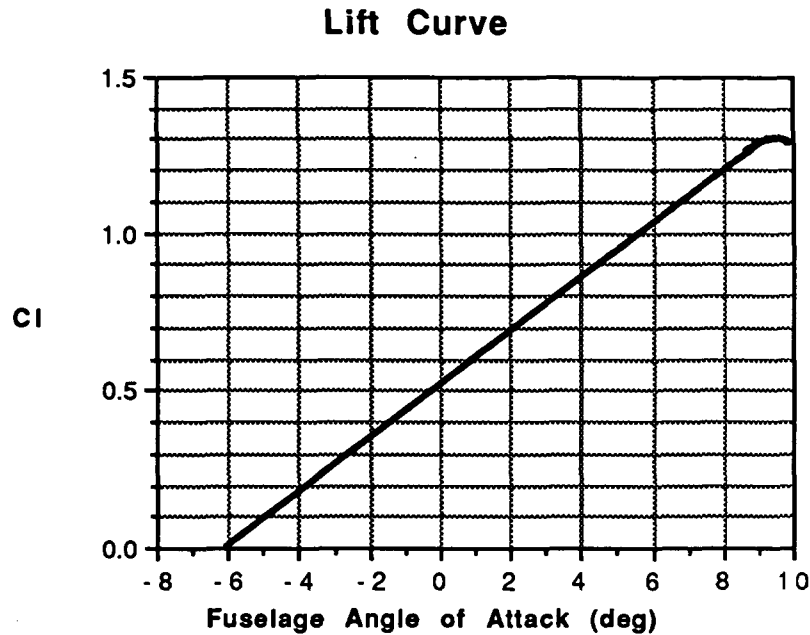
Lift Curve

Figure 2.15 Lift Curve of the *Hotbox*

The maximum lift to drag ratio for the aircraft was determined using the drag polar equation and the fact that at L/D_{max} the parasite drag is equal to the drag due to lift.

$$C_D = 0.034 + 0.05C_L^2$$

from which

$$C_L \text{ at } L/D_{max} = 0.82$$

and

$$C_D \text{ at } L/D_{max} = 0.068$$

therefore

$$L/D_{max} = 12.1$$

From Figure 2-15 it is seen that the lift coefficient (0.82) for L/D_{max} occurs at $\alpha = 3.5°$.

2.6 Influencing Factors

The driving forces behind the aerodynamics design and analysis were:

- ease and feasibility of construction
- cost efficiency in construction and performance
- wing loading

The Spica airfoil provides the *Hotbox* with a wing which is easy and cost effective to construct and which exceeds all performance requirements placed on an airfoil. The proposed wing design incorporates a design with no taper or sweep, again, to aid in construction. Although performance characteristics could improve with the introduction of taper or sweep, the current *Hotbox* performance exceeds all requirements. The cost efficiency drove the design and dominated this decision.

Wing loading was the major consideration in the determination of wing area. Studies of data from last year's projects and other research indicated suggested wing loadings. Because aircraft weight was largely fixed, wing area was set to produce an acceptable wing loading.

In general, drag considerations where outweighed by construction and cost factors. The landing gear, however, was redesigned several times in an attempt to minimize both drag and weight.

3. STRUCTURES AND WEIGHT

3.1 System Requirements

The responsibility of the structures group was to design a fuselage, a wing and an empennage structures which would:

- Result in an aircraft weight of no more than 72 [oz]
- Maintain structural integrity under all normal and maximum expected aerodynamic and inertial loadings.
- Integrate all systems such as lifting surfaces, power plant, control mechanisms, and landing gear.
- Contain a 37 [in] x 5 [in] x 1 5/8 [in] passenger bay housing 40 passengers, a flight attendant, and a galley.
- Have a hinged wing to allow our aircraft with an 8 [ft] wingspan to fit in 5 [ft] gates.

3.2 Materials Selection

The weight requirement made it imperative that strong but lightweight members be used to construct the aircraft. Model-building experience and research on the construction materials used in past years' technology demonstrators, indicated the most appropriate structural materials. These materials are listed in Table 3.1, with their basic properties are:

Material	Density (oz/in^3)	σ_{xx},max(psi)
Balsa Wood	0.0928	5000
Spruce Wood	0.256	6200
Birch Plywood	0.3696	2500
Monokote	1.5-1.75 oz/1000 in2	N/A

Table 3.1 Construction Materials and Common Properties

The Balsa wood is an oriented-fiber material which can carry stress well along the length of its fibers. It has the distinction of being very light-weight. However, it is also very flexible which means that it will buckle under fairly small loads. Figure 3.1 illustrates a quantitative description of buckling and maximum loads for several different common Balsa wood members.

Buckling Force versus Length for Triangular and Rectangular members Balsa
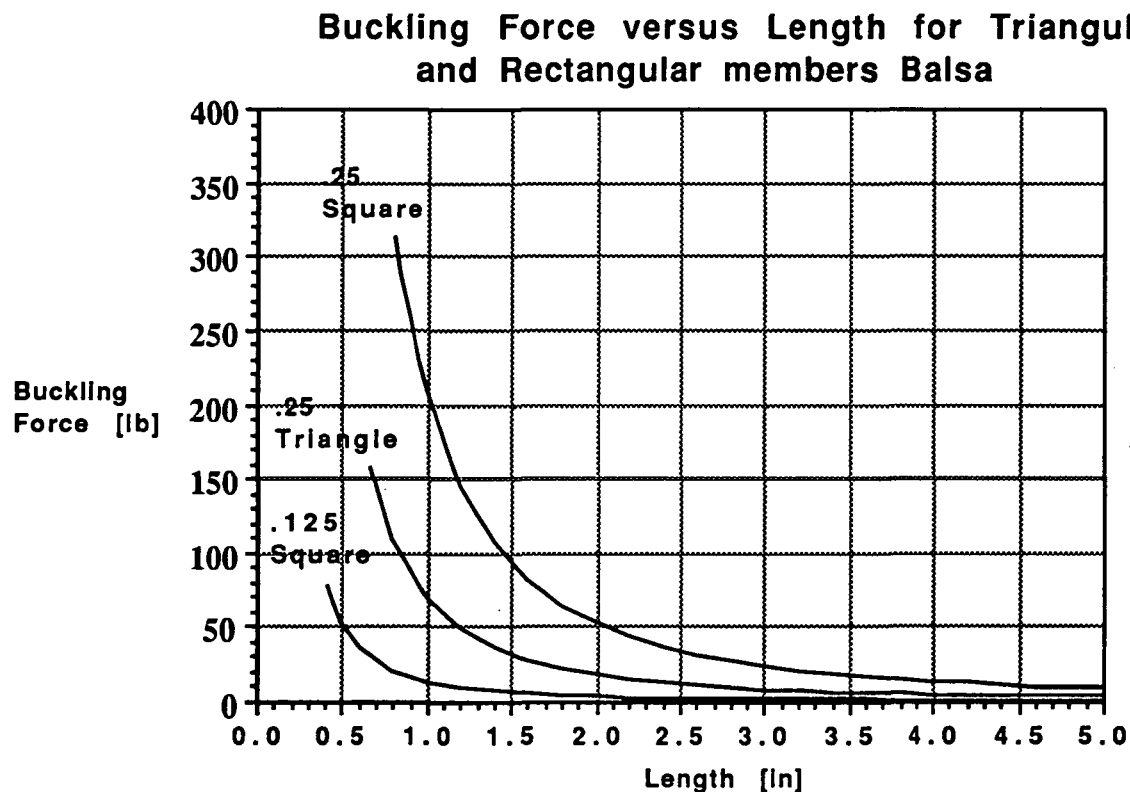
Figure 3.1 Maximum and Buckling Loads for Balsa Wood
(Note: Plots end at fracture strength of various members)

Spruce wood is also an oriented-fiber material which can carry stress well along the length of its fibers. It is about 2.75 times as dense as Balsa, but is also much more rigid than Balsa. This makes spruce a good choice for high-compression

members which cannot be supported well along their length. See Figure 3.2 for a quantitative description of buckling and maximum loads for several different common Spruce wood members.

Buckling Force versus Length for Triangular and Rectangular members Spruce
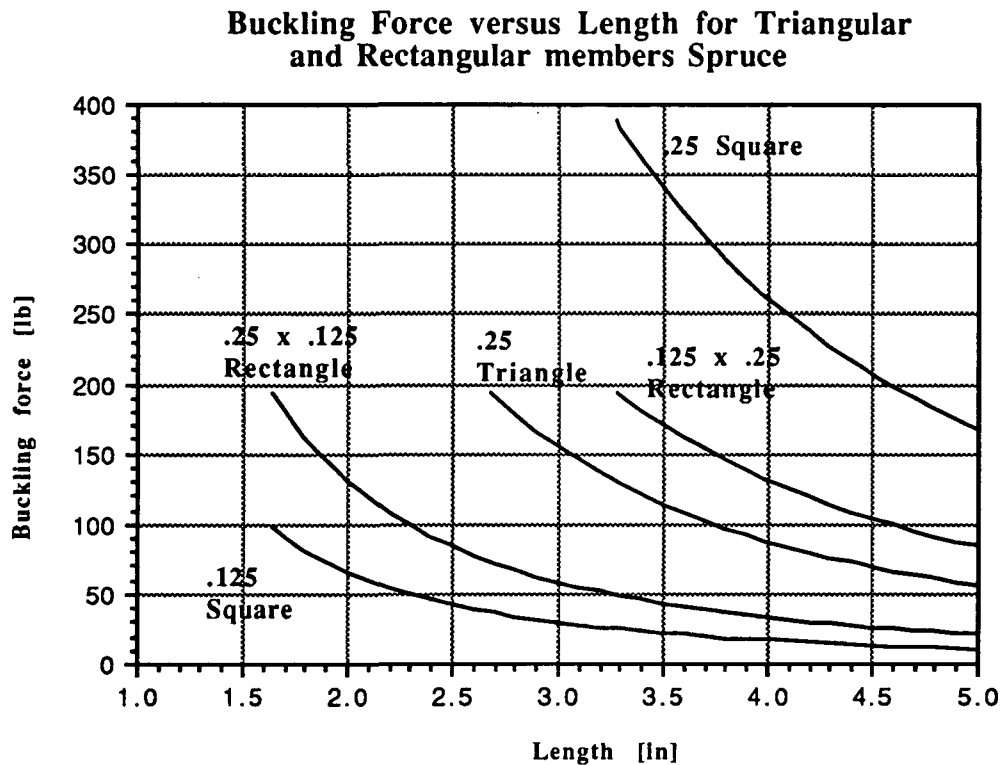
Figure 3.2 Maximum and Buckling Loads for Spruce
(Note: Plots end at fracture strength of various members)

Birch Plywood is also an oriented-fiber material, but it has two different orientations of fibers in it. This allows it to carry fairly high loads along two different (perpendicular) axes. However, these loads are substantially lower than the loads that either Balsa or Spruce can carry along their primary axes. Useful properties of Birch Plywood are that it is very rigid and that it comes in sheets.

Lastly, monokote is a heat-shrinkable, oriented-fiber film which is used as the skin of the aircraft. Several different varieties are available which have different loading, shrinking, and tearing characteristics. Assuming that it is oriented properly (internal fibers perpendicular to shear forces), it can carry relatively high shear loads to help the fuselage and wings resist bending or twisting. The monokote's density is dependent upon its color. Within a given family of monokote film (ie. oriented-fiber film, synthetic fabric, etc.) the chemical composition of the different colors of film is fixed. Differences in density are thus dependent upon the amount of pigment which must be added to achieve desired colors. A substantial amount of pigment must be added to it to create opaque colors. In general, clear Monokote is the least dense while black the most dense.

3.3 Loading Conditions

In order to help determine how loads will be imposed on structural members in flight a V-n diagram was generated. This can be seen in Figure 3.3. It shows the normal and maximum expected aerodynamic loading requirements for the aircraft. The upper load factor limit was based on the maximum expected load in flying at 30 [ft/s] in a 30 [ft] radius vertical loop. The lower load factor limit is based on the maximum expected download the aircraft could generate before stalling the main wing. No gust loads are shown because our aircraft is designed to fly in the still-air environment of Aeroworld, i.e. Loftus Sports Center. Power required plots dictated a maximum speed for the aircraft of 55 [ft/sec], but aircraft in Aeroworld are limited to only 35 [ft/sec]. The *Hotbox* is designed to cruise at 30 [ft/sec]. Other significant aircraft loads are those due to landing and takeoff conditions.
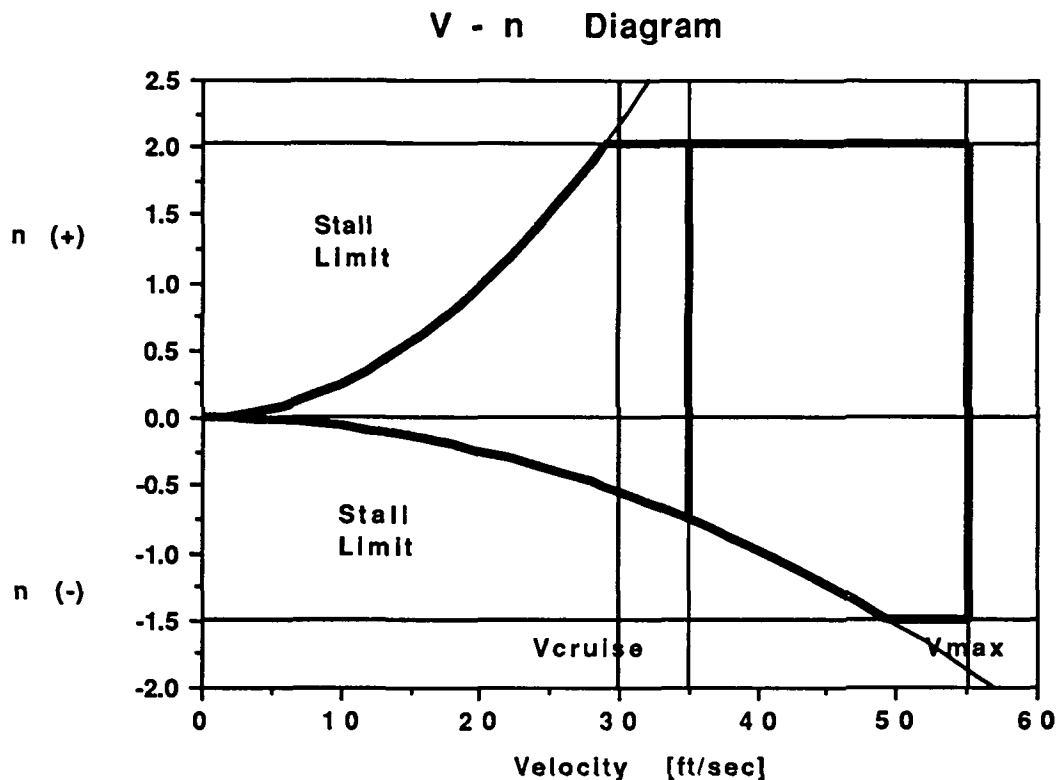
V - n Diagram

Figure 3.3 V-n Diagram

The normal and maximum expected loadings for this aircraft were very important considerations in designing the different required structures. These coupled with the material choices created a large number of structural design possibilities. These, however were limited by the aircraft configuration which our group had already chosen. In the following paragraphs, the design of each of the major aircraft substructures (fuselage, wing, and empennage)will be discussed.

3.4 Fuselage

The most complicated of all of the substructures is the fuselage because it contains so many members. Approximately a dozen different designs were initially created which would meet the loading requirements. These were tested first by hand and then using finite element codes to determine the stresses in each of the structural members. The two different types of designs were the right triangle-based designs and the sawtooth-based designs shown below in Figure 3.4. Stress analysis showed that variations of the right-triangle structure had lower stresses in the members. Because the finite element codes modeled the structural members a pin-ended members and not continuous members, the results are conservative. This means that the predicted stresses in the members are probably higher than would actually be encountered in the structure's members. In addition, the members would be less likely to buckle because they can carry moments at their junctions which the finite element codes do not account for. Thus variations of the right triangle-based structure were considered for the final design, because lower stresses translates to the use of smaller and lighter members.

Sawtooth Type Fuselage Design

Right-Triangle Fuselage Design
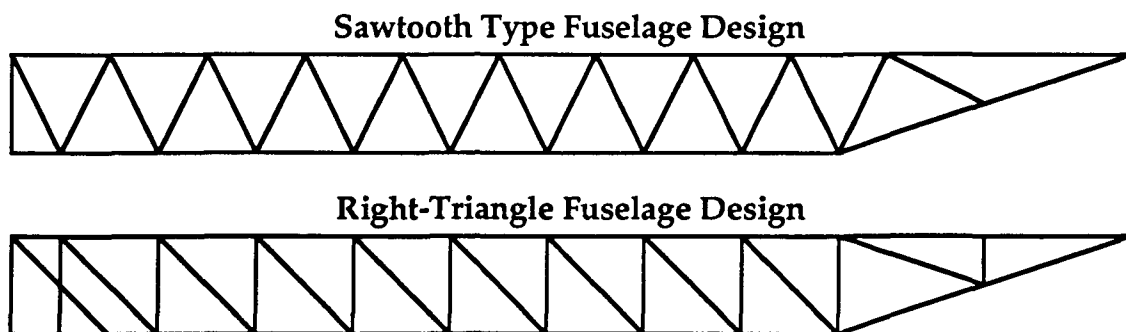
Figure 3.4 Different Fuselage Type Designs

As stated, the first tests concentrated on the stresses in the members and did not concern themselves with the weight of the structure. After determining that a structure could be built which satisfied the loading requirements, weight became the driving factor. This is where the properties of the materials discussed earlier were important. The weight of the aircraft and the location of the different members varied greatly depending upon which material was used. The final determination of the structure design was determined by completely designing three right-triangle based fuselages. The stresses in all of the members were calculated in addition to the location of the center of gravity and the overall weight of the aircraft. These included a mostly Spruce design, a mostly Balsa design, and a design which used about half Balsa and half Spruce. All of these combinations satisfied the loading

←—12 [in] —→
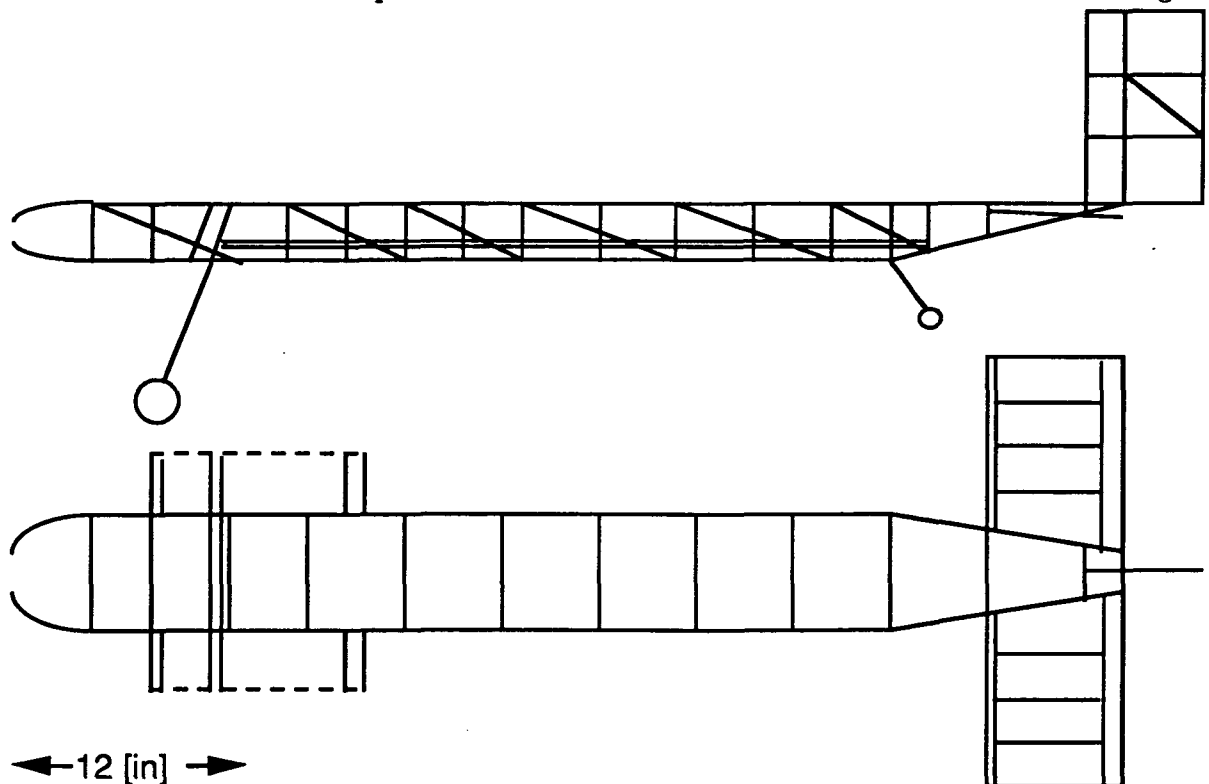
Figure 3.5 Scale Drawing of the *Hotbox*

requirements, but the Balsa design was the lightest. Thus it was chosen as the final fuselage design. Scale drawings of the final design are shown in Figure 3.5 .

Special consideration was given to the internal layout of the aircraft throughout the design process. The aircraft center of gravity had to be located at the 30% chord point and the fuselage had to contain our predetermined seating bay. Other considerations of the internal layout included damping the vibrations of the motor, isolating the speed controller and receiver from motor vibrations, locating the power plant battery for quick removal and replacement, and locating the radio gear for quick access. The final interior layout of the aircraft is shown in the following figure, Figure 3.6.

In general the limiting factor in the design of the aircraft structure was not the ultimate stresses in the members. Although this was important, it was overshadowed by the tendency of the very thin members to buckle. Thus, in the design, the vertical members shown in the side view are more closely spaced toward the nose of the aircraft and more widely spaced near the tail. This is because the internal fuselage moment increases as one moves from the tail to the main wing. The diagonal members aft of the main wing resist both the shearing force between the upper and lower longitudinal members and the internal, vertical fuselage shear force, created by tail and fuselage loadings. The diagonal members forward of the wing support the loads due to the power plant and radio gear. The cross-members,

Internal Layout

1 Motor Battery Pack	6 Motor
2 Receiver Battery Pack	7 Galley
3 Motor Speed Controller	8 Stewardess
4 Servo(s)	9 Passengers
5 Receiver	
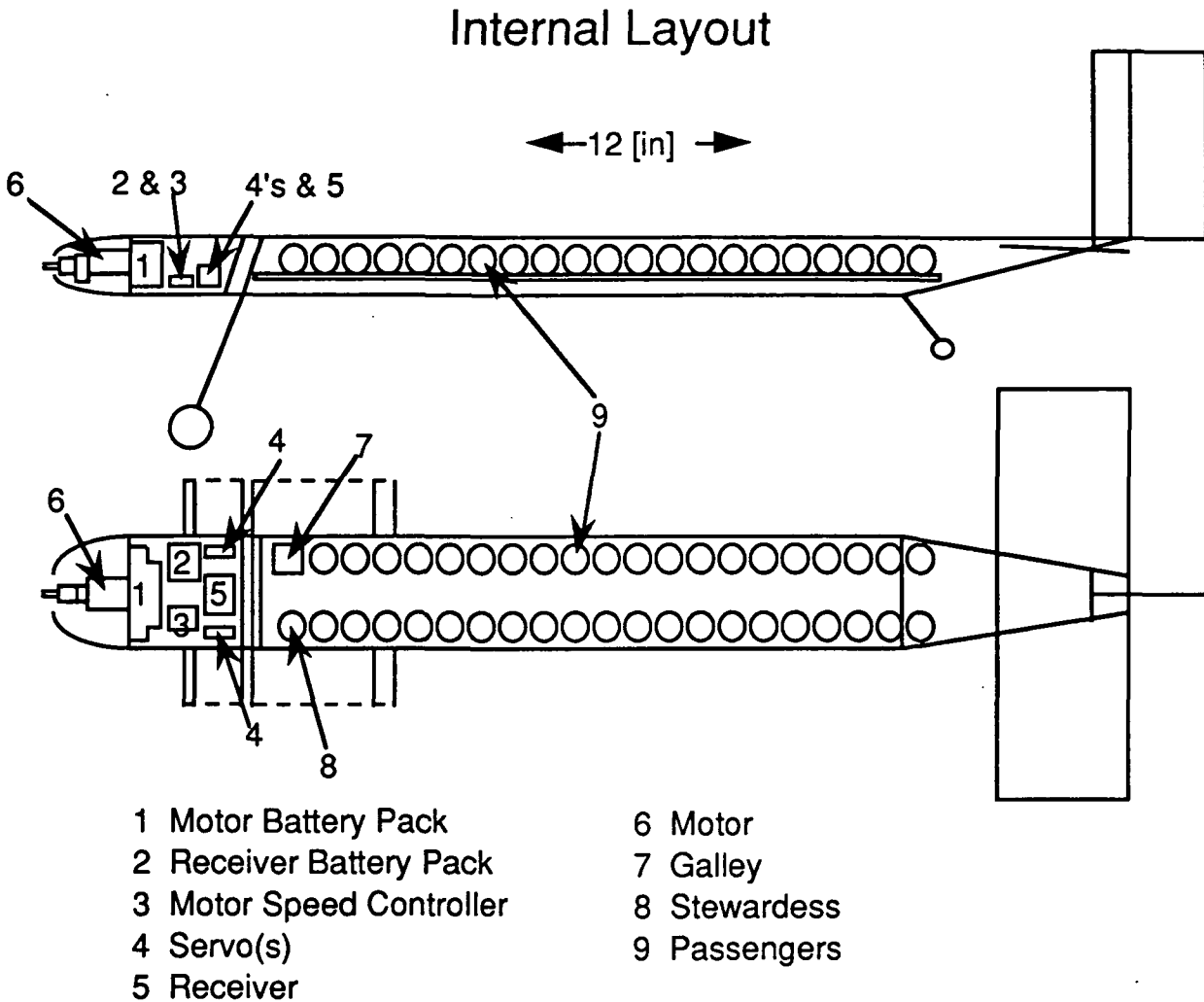
Figure 3.6 Internal Configuration of the *Hotbox*

shown in the top view of Figure 3.5, help the longitudinal members hold their shape and resist buckling when the Monokote is shrunk around the fuselage structure. Monokote is used to help the fuselage resist twisting due to vertical tail loads in addition to providing a smooth exterior surface. Note that the heavy items such as the motor, power plant battery, and radio gear are located near the nose of the aircraft to pull the aircraft center of gravity forward to the desired 30% chord point. Note also that all of these heavy items are located close to where the wing

and the front landing gear attaches to the fuselage. Such an arrangement helps reduce the structure necessary to transfer the loads (due to these heavy items) to the wing and the landing gear. This is critical because the wing and landing gear support the weight of the aircraft during various phases of operation. The following table, Table 3.2, lists the key design parameters of the fuselage.

Length of Fuselage	57.0 [in]
Total Length of Aircraft	61.5 [in]
Width(max)	5.5 [in]
Width(min)	1.0 [in]
Height	2.75 [in]
Weight	7.83 [oz]

Table 3.2 Fuselage Design Parameters

3.5 Wing

The next substructure, in order of complexity, was the wing. For the reasons discussed in the aerodynamics section, the wing has: a rectangular planform, an 8 [ft] span, an 11 [in] chord, no sweep, and 7° of dihedral. The rectangular planform and lack of sweep made the design process very straight-forward. Monokote is used to cover the wing and control wing twisting and fore-aft deflections due to drag and landing forces. The internal wing moment and shear forces are controlled by a .125 [in] x .25 [in] spruce spar on the top and bottom of the quarter-chord point. In addition there are also spars running the full length of the wing at the leading and trailing edges. These help carry some of the aerodynamic loading in addition to defining the leading and trailing edge shapes of the wing. The shape of the wing

cross-section is defined by balsa airfoil sections which run from the leading to trailing edges of the wing. They are placed at 4 [in] intervals and have lightening holes drilled in them. See the following figure, Figure 3.7 for a drawing of the cross-section of the wing.
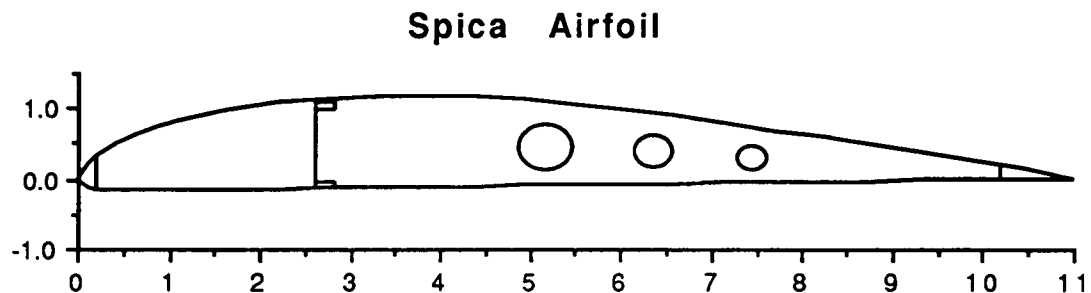
Spica   Airfoil

Figure 3.7 Cross Section of Spica Airfoil with lightening holes

Note that the entire airfoil surface is convex which allows Monokote to be attached easily. A 0.0625 [in] thick Birch plywood sheet is attached to the front of the upper and lower quarter-chord spars to form a web between them. This keeps the upper and lower quarter-chord spars from shifting with respect to each other and provides additional wing stiffness.

Following is a planform view of the wing with the leading edge at the top of the page and the inboard side of the wing to the right. It shows the basic construction of the wing
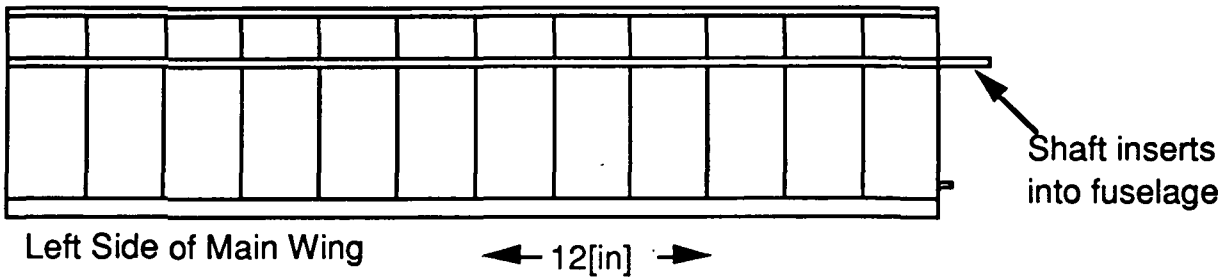
Figure 3.8 Planform View of Wing

In order to reduce drag, the wing is mounted on either side of the fuselage 7.125 [in] aft of the nose of the aircraft, rather than on the top of the aircraft. The wing is not continuous through the fuselage. Both halves (right and left) of the wing have extensions of their quarter-chord spars which insert into a box structure in the fuselage. The moment generated by the wing is transferred to the fuselage by a peg at the rear of the wing.

One of the most significant aspects of this wing is that it is hinged to allow the aircraft to service 5 [ft] gates. The primary hinge mechanisms are located at the quarter chord, 26.75 [in] out on either side of the wing to transmit the lift, drag, and moment, generated by the outboard side of the wing, to the inboard side of the wing. The hinges are located between the upper and lower spars on the inboard side of the wing. When the wing needs to be folded, the hinge slides out and folds up. A peg is located near the trailing edge of the airfoil sections on either side of the wing's hinge point. This peg helps transmit the moment generated by the outboard side of the wing. In addition, the peg is designed to support the wing while it is folded in its up position. The maximum expected internal wing hinge moment is 30 [in-lb]. This causes a maximum stress of 720[psi] in the hinge which is made of a 1[in] x 0.25[in] piece of spruce. 720[psi] is only 12% of the spruce's maximum stress of 6200[psi] and the hinge is not in danger of buckling. Hinge construction tolerances do not seem to

pose a serious problem. All pieces of the hinge will be carefully assembled to ensure that the wing does not deflect more than one additional degree of dihedral under extreme loadings due to hinge deflection. See the following figure, Figure 3.9, for more details on the basic construction and operation of the wing hinge.

Wing Hinge in Unfolded Position

Outboard side
of wing

Inboard side
of wing

Quarter-Chord Spruce spars

Hinge
Fixed
to wing
on this
side of
wing

Wing Hinge in Folded Position

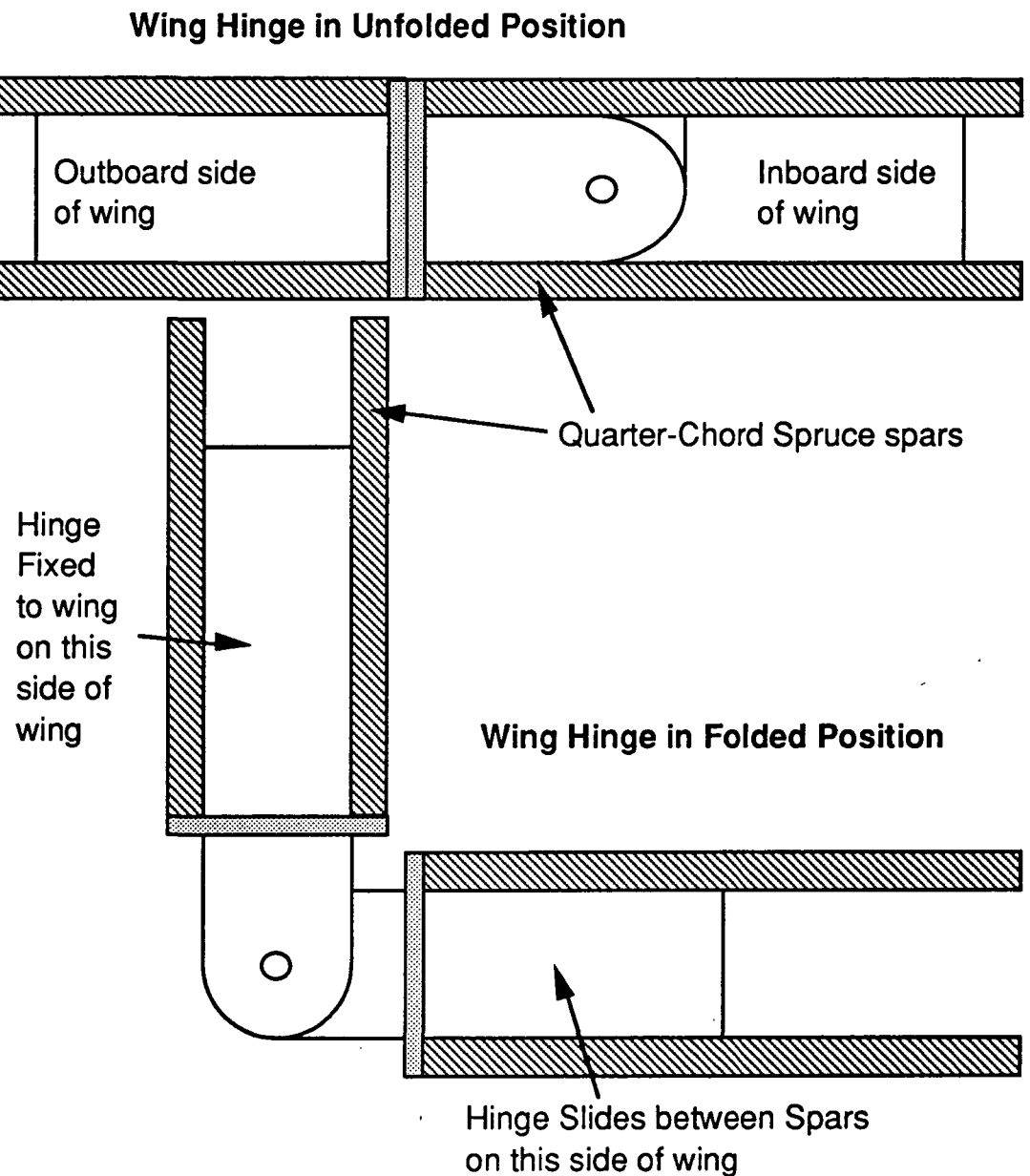Hinge Slides between Spars
on this side of wing

Figure 3.9 Wing Hinge

3.6 Empennage

The last substructure of the aircraft to be designed was the horizontal and vertical tails (by virtue of the fact that the maximum loadings on these portions of the structure were determined late in the design process). Both tails were very simple to design. They both have rectangular planforms with simple hinged flaps at their trailing edges. Like most of the remainder of the aircraft, they are built entirely of Balsa wood and covered with Monokote. The Monokote will also be used for the hinge material. This eliminates the gap between the fixed and movable parts of the tails and helps to keeps the entire tail surface more rigid. See Figure 3.5 for drawings of the horizontal and vertical tails.

After the designs for the fuselage, wing, and empennage were completed, the entire aircraft was ready for assembly on paper. Care was taken to ensure that all systems had proper space, and clearances. In addition the aircraft c.g. had to be precisely located at the 30% chord point. Our calculations, however showed that the aircraft c.g. actually lay ≈1.5 inches behind that point. Thus, the nose of the aircraft was lengthened by 2 [in] to cantilever the motor and battery packs out a little further to the front. This modification placed the aircraft c.g. exactly where it needed to be and created more room for the radio and power plant equipment. A weight penalty of ≈0.15 [oz] was incurred, but this was deemed a reasonable tradeoff for properly locating the c.g.

3.7 Landing Gear

A significant design feature of The *Hotbox* was the design and selection of the landing gear. Preliminary design requirements established that the Hotbox would

use a taildragger configuration to ensure stability on the ground. Beyond that configuration requirement, the landing gear was only required to maintain the nose of the aircraft at least six (6) inches (maximum propeller diameter) off the ground to ensure that contact was not made between the propeller and ground during landing. These two requirements drove landing gear design.

Figure 3.10 summarizes the height requirements for the front struts.
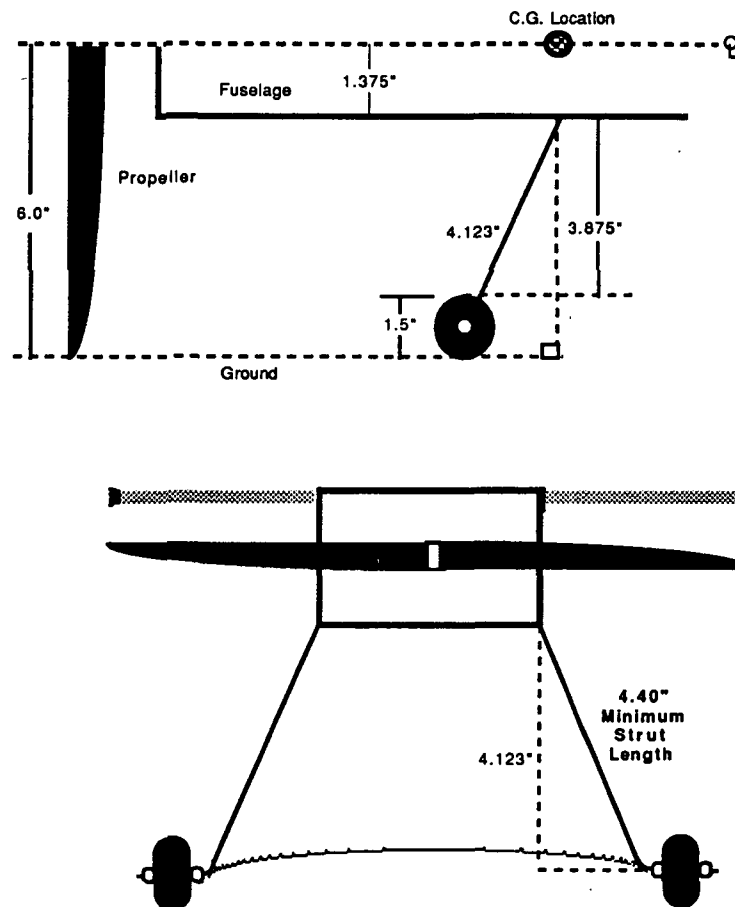

Figure 3.10 Height Requirements

It was found that the landing gear must maintain a length of at least 4.40 inches upon landing to ensure that the propeller did not impact the ground. A propeller diameter of 12 inches had been specified during the propulsion system selection and it was for this diameter that the landing gear was sized. The propeller lies on the centerline of the 2.75 inch fuselage which provides 1.375 inches of propeller diameter not included in strut length. The diameter of the wheels also reduced the required strut length by .75 inches. The remaining length to the ground is the minimum 4.40 inches mentioned previously.

For the analysis that follows it was assumed that the landing gear struts could be modeled as a cantilever beam with a concentrated load applied at one end. It was also assumed that the load applied in landing is small enough such that only elastic deformation occurs. Further, it was assumed that there was no deflection of the tires on landing. A generic but handy Microsoft Excel® spreadsheet was created to determine the deflection of a cantilever beam to a load applied at the end. The equation for maximum deflection may be written:

$$x = \frac{PL^3}{3EI}$$

where L=length, P=applied load, E=Modulus of Elasticity, and I=moment of inertia of the beam. I was calculated for each desired radius using

$$I = \frac{\pi r^4}{4}$$

where r=radius. The worksheet asks for beam length and the modulus of elasticity and density of the strut material. For specified radii and applied loads, the spreadsheet calculates the maximum deflection of the strut as well as its weight.

The front struts of the landing gear will consist of 6.0 inches long, 3/32 inches diameter solid steel tubes. Predictions indicate that the struts will deflect no more than 1.75 inches. The geometry specifies that the gear should not be allowed to

deflect any more than 1.24 inches. To ensure that deflection beyond 1.0 inches does not occur, a steel wire will be attached to the struts at the point of wheel attachment. The wire will contain 1 inch of slack in the system which will allow the struts to deflect up to 1 inch. The wire will not allow deflections beyond 1 inch. This will also aid in maintaining rigidity in the system during taxi starts such that the *Hotbox* will not bounce on the struts during power up.

The front wheels will be foam type, non-tread tires. These are a light weight alternative to the common rubber tires. The wheel width should be large enough such that the wheels will not stick in the Astroturf runway surface. As specified earlier, the wheels will be of a 1.5 inch diameter.

The selected airfoil for the *Hotbox* requires mounting at an incidence angle of 5° and for takeoff it was desired that the wing be at an angle of 9°. Therefore, the remaining 4° was to be provided using the tail gear. This implies that the fuselage and consequently the passenger compartment will be at the slight angle of 4°. This was considered acceptable. The rear gear consists of a 1/16 in. strut and non tread tire similar to those used for the front gear. The deflection on landing will not be as severe as that on the front gear, and some deflection will even help in preventing the propeller from impacting the ground. When the rear strut deflects, the nose of the aircraft will raise slightly, lessening the possibility of impact.

The final configuration for both the front and rear gear are illustrated in Figure 3.11. The analysis performed has allowed for confident selection of the materials and size of the struts to ensure that the landing gear meets the design requirements assessed to it.

C.G. Location

Fuselage

Propeller

Landing Gear Strut
6.0 in. Length
3/32" Diam.

1.5 In. Diameter
No-Tread Tire

Landing Gear Struts
6.0 in. Length
3/32 in. Dia.

Steel Support Wire w/ 1" Slack
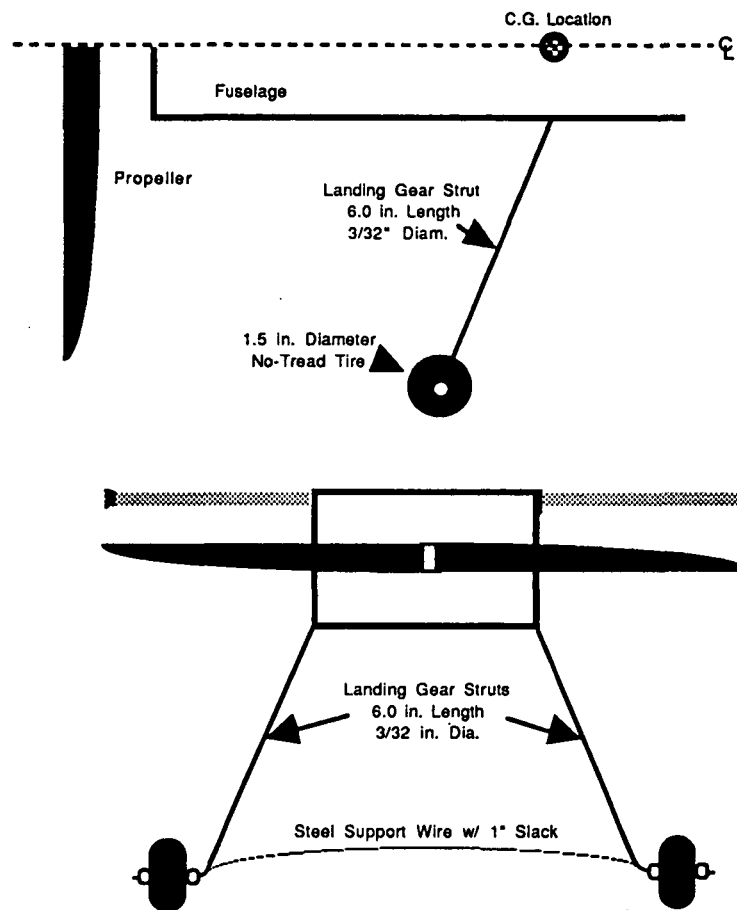
Figure 3.11a Front Landing Gear Configuration
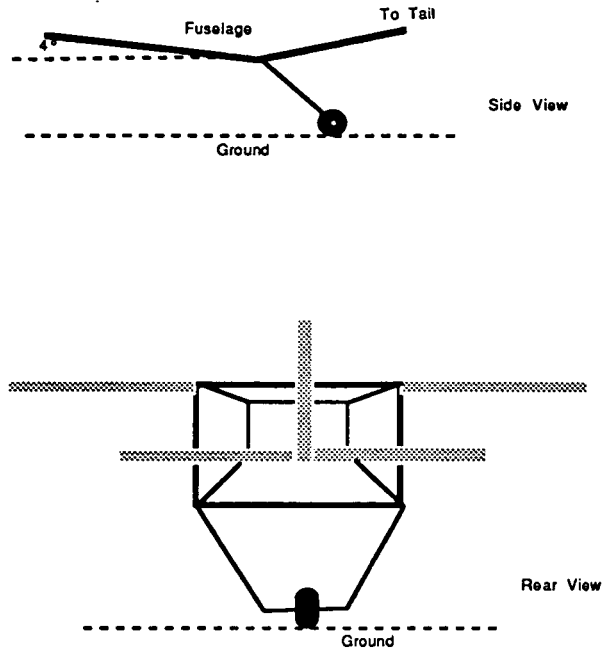
Figure 3.11b Rear Landing Gear Configuration

3.7 Conclusion

The final sub-system weights are listed in Table 3.3:

Sub-system	Weight	X-location	Z-location
Fuselage	7.83	26.54	2.46
Nose Fairing	0.5	2.5	1.375
Landing Gear	3.0	20.0	-3.3
Power Plant	13.71	3.14	1.38
Battery	17.8	5.03	0.378
Radio Gear	6.84	12.44	1.38
Wing	13.2	9.64	4.8
Passengers	3.7	29.5	1.5
Glue	≈2.0		

Total Aircraft Weight: 68.6 ozs

Table 3.3 Subsystem Weight Breakdown and Center of Gravity Location
(Note: Some numbers are shown with more significant figures than others because they can be more accurately calculated than others.)

The desired aircraft c.g. is 10.43 [in] aft of the nose of the aircraft. The actual c.g. location can travel from 9.5 [in] (with no passengers) from the nose to 10.6 [in] (with a full load of 40 passengers) from the nose.

Thus, both the total weight and range of c.g. travel meet our design requirements. Over the course of the design project, these two numbers were the biggest challenge associated with the aircraft structure.

4. PROPULSION

Motor Type	Astro 15
Propeller	Top Flight 12-6
Number of Batteries	9
Battery Pack Voltage	10.8 V
Battery Capacity	1200 mah

Table 4.1 Summary of Performance System Characteristics

4.1 System Requirements:

Early in the design process the mission was defined and several propulsion system requirements followed from the mission objectives. The propulsion system is required to:

- Utilize a single electric powered engine
- Provide sufficient power for takeoff within sixty (60) feet
- Supply power for a 5500 ft minimum flight
- Sustain steady level flight at a velocity of 30 ft/s

Selection of the appropriate motor followed.

4.2 Motor Selection

The use of an electric powered motor was specified in the Request for Proposals (see Appendix 1). A single engine design was selected due to the added complexity and weight associated with a multi engine design. The added cost of the propulsion system associated with multiple engines was also deemed to be unnecessary.

The electric motors evaluated included the Astro 035, Astro 05, Astro FAI05, and the Astro 15. From initial estimates of motor power requirements, it was concluded that the Astro 035 was inadequate. It was not capable of producing the necessary power to fulfill the mission requirements.

The Astro 035 was eliminated from further consideration. Attention then focused on the Astro 05's and the Astro 15.

Meeting the takeoff distance requirement was the driving influence behind propulsion system selection and was thus crucial in motor selection. Takeoff was to be achieved in less than 60 ft (see section 1.3). Preliminary power production estimates showed that both motors could exceed the estimated power required but the Astro 15 had greater excess power which would aid in takeoff and even displayed greater range capabilities by several thousand feet. The Astro 05 could not meet the takeoff distance requirement in this early investigation. Finally, the weight of each motor was investigated. The Astro 05 weighed only 1 ounce less than the Astro 15, however this did not include battery weight. Using the manufacturers recommended battery pack size, it was found that the Astro 05 motor and battery system weighed 9 ounces less than that of the Astro 15 with its associated battery pack. At that stage in the design process, weight rationing had not been imposed and the 9 ounce weight penalty would be accepted in order to ensure meeting the takeoff distance requirement. The Astro 15 Cobalt Motor was selected.

4.3 Propeller / Battery Selection

While analyzing the Astro 15, an investigation into the performance characteristics of propellers was initiated to determine the most appropriate propeller for meeting our requirements. It was first necessary to determine the propeller performance characteristics (thrust coefficient, C_t and power coefficient, C_p) as a function of the advance ratio, J. These characteristics were obtained using a program entitled "Notre Dame Propeller Program," written by Barry Young. This code allowed for generation of theoretical propeller

performance characteristics based on simple blade element theory. Blade section airfoil data, flight conditions, blade angle, chord, and thickness were provided as input. The program assumed that all propellers used the Clark Y airfoil as this was the default in the program. It was also assumed that the only geometrical difference between propellers of the same diameter but varying pitch was the blade angle at each radial position.

The analysis of the propeller data included diameters of 8, 10, and 12 inches and pitches of 4 and 6 inches. Overall, six propellers were combined with the Astro 15 motor powered by battery pack voltages of 9.6, 10.8, 12, 13.2, 14.4, and 15.6 to determine the best engine / propeller / battery package for The *Hotbox*. The Fortran code written by Prof. S. Batill, Takeoff Performance, computed the performance characteristics for takeoff given detailed propeller performance data (from Barry Young's program). Results are shown in the graph of takeoff distance vs. battery voltage (Figure 4.1).
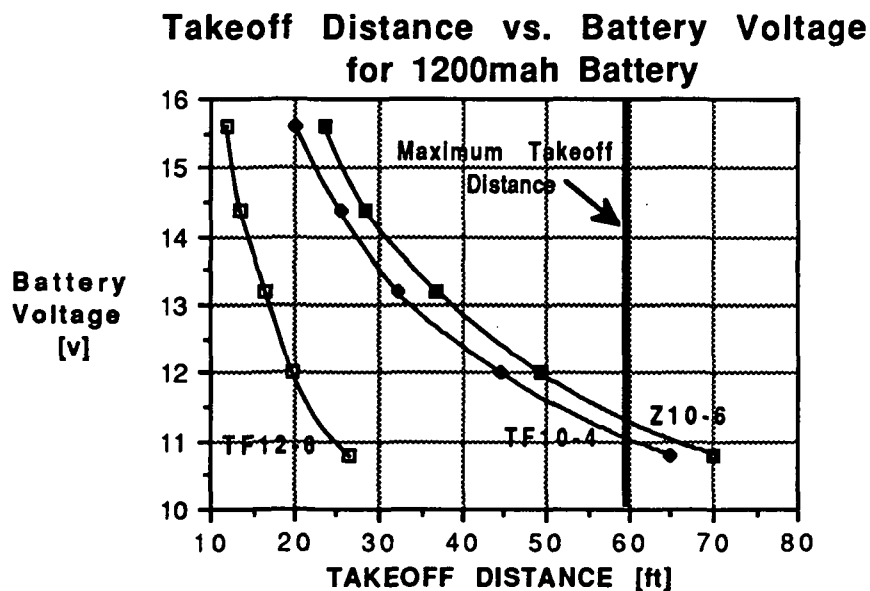
Figure 4.1 Takeoff Distance vs. Battery Voltage

This graph shows that the Top Flight 12-6 Propeller was the only propeller to takeoff within the required distance using a battery voltage of 10.8 volts. The other propellers could have met the takeoff distance requirement had a greater battery voltage been used. However, increasing the battery voltage requires increasing the number of batteries which results in a weight penalty. At this stage in the design process, minimizing the weight of the aircraft and consequently the propulsion system became important. Since the motor had already been selected, the battery pack was required to be as lightweight as possible while still meeting all design requirements. The Top-Flight 12-6 required a pack voltage of 10.8 at a weight of 15.3 oz. This was the minimum required pack weight for all competing propellers.

Each propeller was also evaluated on the basis of power available vs velocity, shown in Figure 4.2.

Power Available vs Velocity for Tested Propellers and Astro 15
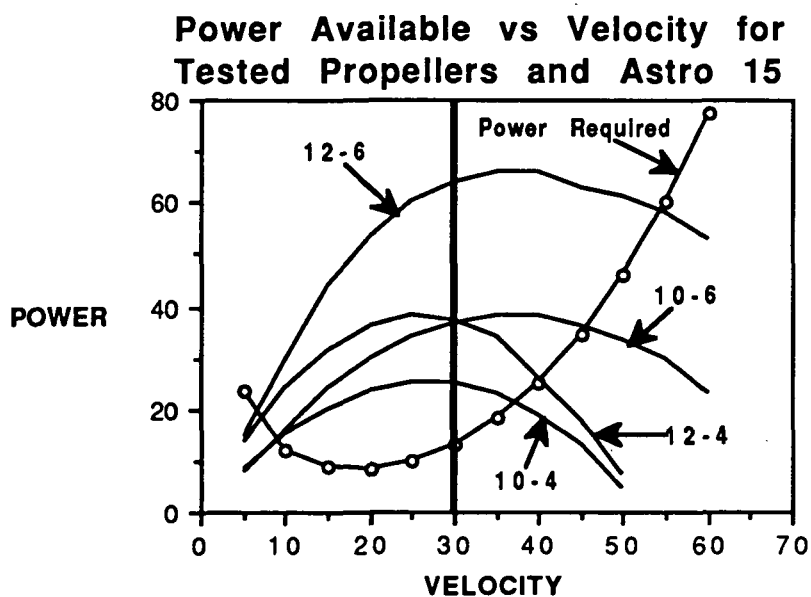
Figure 4.2 Power Available vs. Velocity

The Top Flight 12-6 clearly provides the maximum power available of all the competing propellers. The TF 12-6 therefore maximizes excess power and subsequently rate of climb. The 12-6 enables the aircraft to climb to our design altitude of 20 ft in 2 seconds versus greater than 5.5 seconds for the next best propeller, the Top Flight 12-4. A plot of the efficiency versus advance ratio for the 12-6 is given in Figure 4.3. Cruise efficiency is indicated on the curve as 0.716.

**Efficiency vs Advance Ratio
Top-Flight 12-6 Propeller**
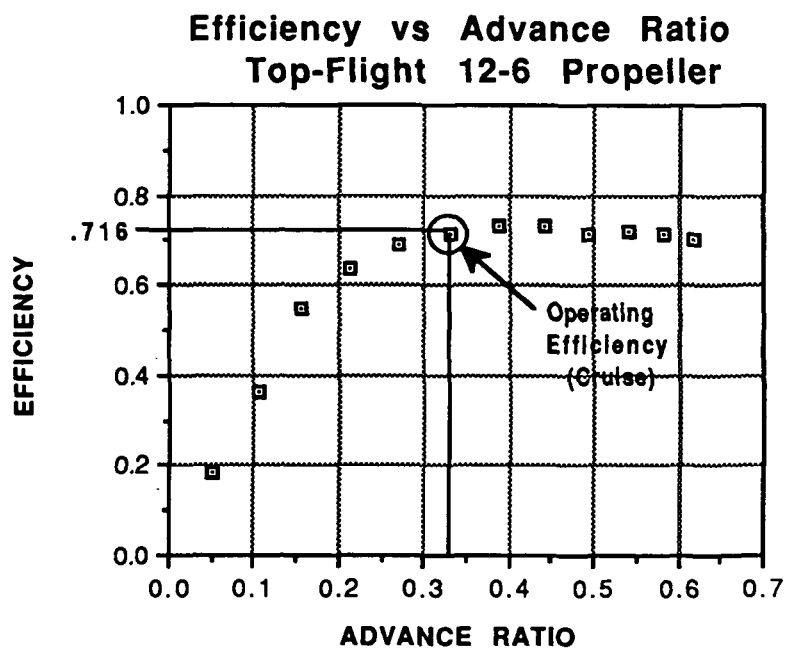
Figure 4.3 Efficiency v. Advance Ratio

It was also necessary to calculate the expected range for the Astro 15 motor fitted with competing propellers and Figure 4.4 compares the various propellers in range vs velocity.

The figure shows that the 12-6 provides the minimum range of the group, but it still far exceeds the minimum range requirement set in the mission definition. As stated in the mission definition, fuel efficiency was a driving concern in technical decisions, wherever possible. In this instance,

cruise fuel economy could have been better served with a different propeller. However, in order to meet maximum weight requirements, battery weight was reduced. With fewer batteries, battery voltage is reduced. At the reduced battery voltage, only the 12-6 could achieve take-off. Thus, economic considerations were outweighed.

Range vs Velocity for Tested Propellers
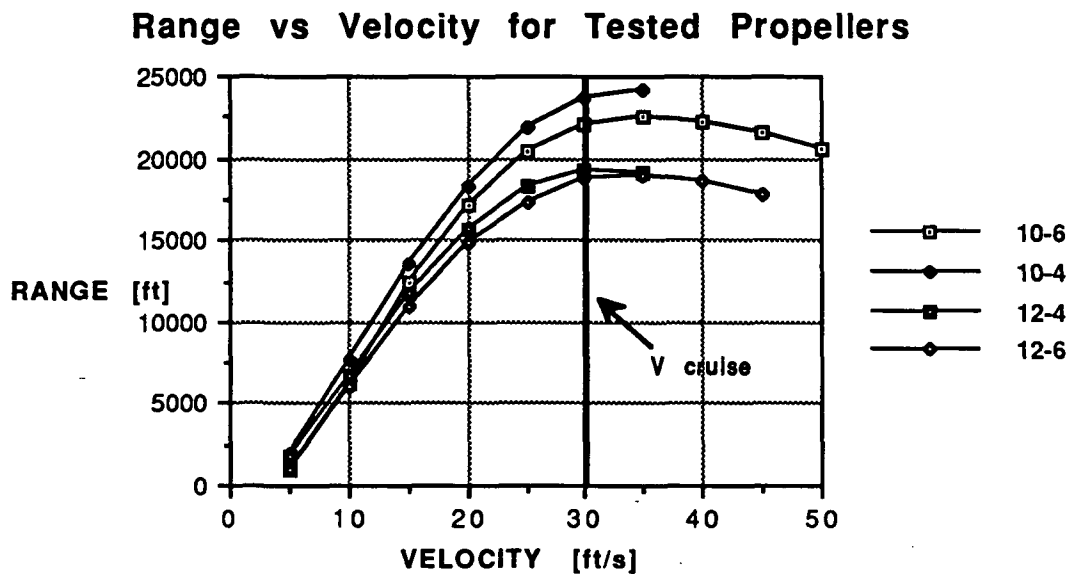
Figure 4.4 Range vs. Velocity

The final aspect of the propulsion system selection was battery sizing. As was specified earlier, a battery voltage of 10.8 volts was selected as it allows for meeting the takeoff distance requirement using a minimum battery weight. In order to further reduce the weight of the battery pack, an investigation was conducted into using lighter 800 mah batteries instead of 1200 mah batteries. Overall, a 5% weight penalty was associated with using the 1200 mah battery. However, this 5% weight penalty resulted in a 50% increase in range. This allows for multiple flights without changing

refueling. Thus, the weight penalty was judged to be outweighed by the range benefit.

4.4 Speed Control

The propulsion system will also incorporate a speed controller in order that the pilot may throttle back the motor after takeoff to achieve steady level flight at cruise. The takeoff and climb phases of the mission will be performed at full throttle. Reducing the throttle during cruise will allow for a reduction in battery consumption in order to increase endurance. Examination of existing data suggested that the pilot will be required to throttle back approximately 40% after the climb phase. This will allow the pilot to maintain steady level flight during cruise. The pilot will, however, need to throttle up during turns to maintain altitude. This is due to the fact that turning through the use of dihedral and rudder deflection in place of ailerons causes the aircraft to loose altitude during a turn. The pilot must increase the velocity of the *Hotbox* to 32 ft/s in a turn to ensure that the component of lift in the vertical direction remains constant and thus avoid losing altitude. The other option would be to increase the angle of attack, but, this would also increase drag.

Meeting the takeoff distance requirement and weight reduction were the driving factors behind propulsion system selection. The propulsion system consists of the Astro 15 motor and Top Flight 12-6 powered by nine 1.2 volt, 1200 mah batteries and a speed controller. This system was selected because it provides The *Hotbox* with the propulsion system best suited to meeting its design requirements.

5. STABILITY AND CONTROL

5.1 System Requirements

In order to successfully fly an aircraft, it is necessary for the aircraft to be stable and controllable. The main control requirements for the *Hotbox* were:

- Maintain steady level flight.
- Longitudinal stability to be accomplished with a horizontal tail.
- Lateral Stability to be accomplished with a vertical tail.
- Pitching motion to be controlled by elevator deflection.
- To be able to negotiate the turns in the course though a combination of wing dihedral and rudder deflection.

This section outlines the design procedures used in meeting these control objectives.

5.2 Static Margin

The static margin is an important parameter in determining the longitudinal stability of the aircraft. A typical value of the static margin is between 5% and 10% for conventional aircraft. Due to the fact that the pilot of an RC aircraft is on the ground and not in the aircraft, a larger static margin was needed due to the longer response time involved with a ground-based pilot. The static margin for this aircraft was chosen to be 15% of the mean aerodynamic chord. The static margin is defined by:

$$\text{Static Margin} = \frac{X_{np}}{c} - \frac{X_{cg}}{c}$$

Because it was desirable for the neutral point location to be 4.95 inches aft of the leading edge of the wing, 45% chord, and the center of gravity is located at 30% chord, the static margin was determined to be 15% of the chord. The neutral point is significant because it is the furthest aft location of the center of gravity. If the center of gravity is located at the neutral point, the aircraft

will be neutrally stable. If the center of gravity is aft of the neutral point, the aircraft will be statically unstable. The aircraft is statically stable if $C_{m\alpha}<0$. The neutral point is the center of gravity location at which the value of $C_{m\alpha}=0$. $C_{m\alpha}$ is defined as:

$$C_{m\alpha} = C_{L\alpha w}\left(\frac{X_{np}}{c}-\frac{X_{cg}}{c}\right)+C_{m\alpha f}-\eta V_h C_{L\alpha t}\left(\frac{1-d\epsilon}{d\alpha}\right)$$

where $C_{m\alpha f}$ is given by:

$$C_{m\alpha f} = \frac{1}{(36.5Sc)}\sum\left[w_f^2\frac{d\epsilon_u}{d\alpha}\Delta x\right] \quad \left\{\frac{1}{deg}\right\}$$

This value can be calculated from the geometry of the aircraft and the plot of $d\epsilon_u/d\alpha$ in Figure 2.12 of Reference [5]. Setting $C_{m\alpha}=0$ and solving for X_{cg} yields:

$$\frac{X_{np}}{c} = \frac{X_{ac}}{c}-\frac{C_{m\alpha f}}{C_{L\alpha w}}+\eta V_h\frac{C_{L\alpha t}}{C_{L\alpha w}}\left(1-\frac{d\epsilon}{d\alpha}\right)$$

This location is the stick fixed neutral point. This result is based on the assumption that the difference between the vertical positions of the aerodynamic center of the wing and the center of gravity is negligible. This is a reasonable assumption for the *Hotbox*; therefore, the drag contribution to the moment coefficient can be neglected.

5.3 Longitudinal Stability

In order for an aircraft to be longitudinally stable, it must be able to trim at the desired angle of attack. An aircraft is trimmed if the moment coefficient for the entire aircraft at the given angle of attack is zero. Each

component of the aircraft, the wing, fuselage, and horizontal tail, contribute to the moment coefficient. As stated earlier, the slope of the moment coefficient vs. angle of attack curve must be negative for the aircraft to be statically stable. Since the aircraft must be able to trim at cruise where the wing is at a positive angle of attack of $5°$, C_{mo}, the moment coefficient at zero angle of attack, must be positive. However, for the fuselage/wing combination, $C_{m\alpha}>0$ and $C_{mo}<0$. Both of these values are unacceptable for stability requirements. The objective is therefore to determine the area and incidence angle for the horizontal tail in order to provide adequate static stability. The expression for the moment coefficient for the entire aircraft was given in the previous discussion about the static margin. This relationship is represented graphically in Figure 5.1 showing the moment coefficients for the various components and the entire aircraft.

Moment Coefficient vs Angle of Attack
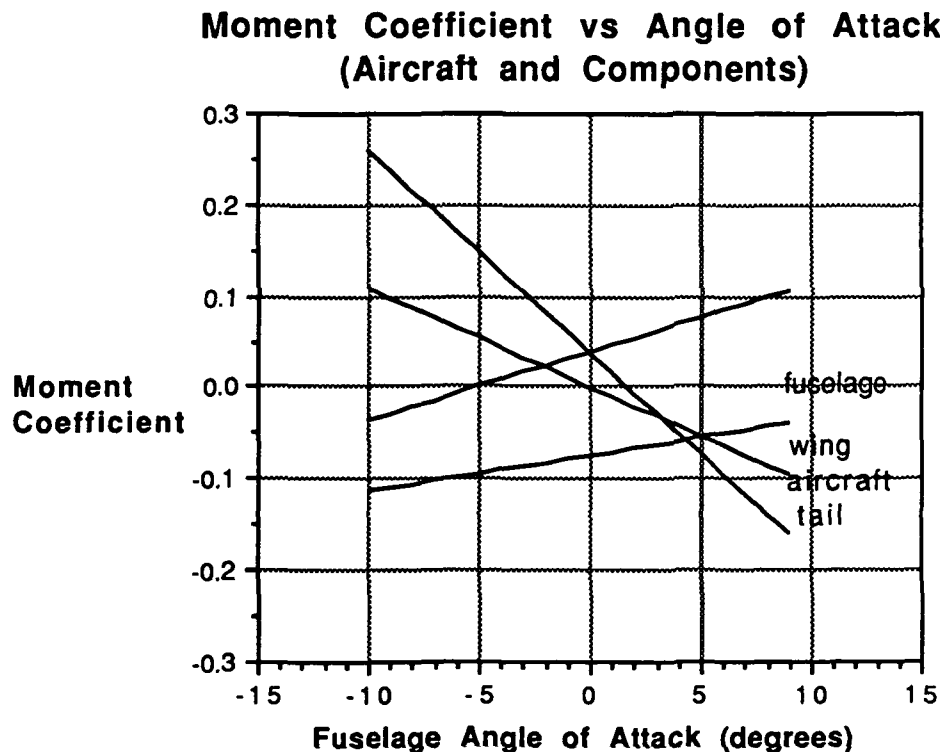### (Aircraft and Components)

Figure 5.1 Graph of Moment Coefficient for Aircraft and Components.

The horizontal tail contribution to the moment coefficient is influenced by a number of design parameters including the center of gravity location, $C_{L\alpha t}$, the horizontal tail area, the horizontal tail incidence angle, the wing incidence angle, the distance from the center of gravity to the aerodynamic center of the horizontal tail, and the cruise conditions. Many of these parameters are already known from other considerations. As was stated earlier, it is known that the center of gravity for the *Hotbox* is at the 30% chord location. From the wing design, it is known that the wing incidence angle is 5°. From the configuration of the aircraft, the distance from the center of gravity to the aerodynamic center of the horizontal tail is also set. The cruise conditions are also known from the design requirements and objectives.

A *TK Solver* routine was used to determine the horizontal tail area and incidence angle required to provide sufficient statical stability. The horizontal tail area was dictated by the static margin and tail moment arm in order to yield a desirable $C_{m\alpha}$. As shown in Figure 5.2, the tail area required decreases as the moment arm increases. This figure also shows that the tail area required increases with increasing static margin. This is because the aft most center of gravity location moves back as the static margin increases which decreases the distance from the center of gravity to the aerodynamic center of the tail. This shortening of the tail moment arm increases the horizontal tail area needed for stability.

The airfoil section of the horizontal tail was also considered as part of the design process. Figure 5.3 shows the effect of $C_{L\alpha t}$ on the horizontal tail area.

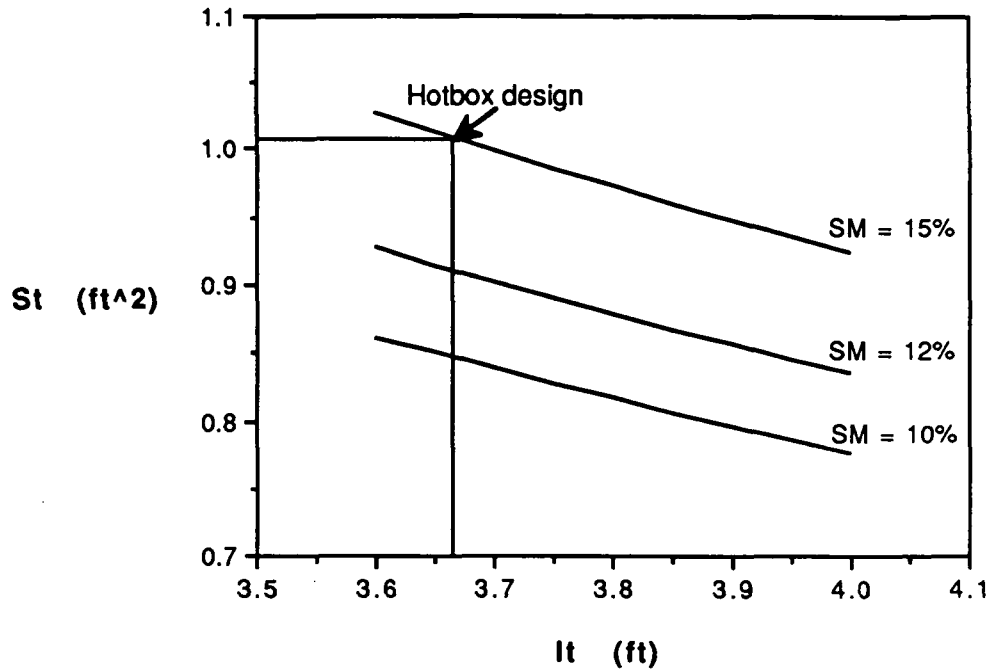## Horizontal Tail Area vs Moment Arm (varying Static Margin)

Figure 5.2 Graph of Horizontal Tail Area vs. Moment Arm Varying the Static Margin.

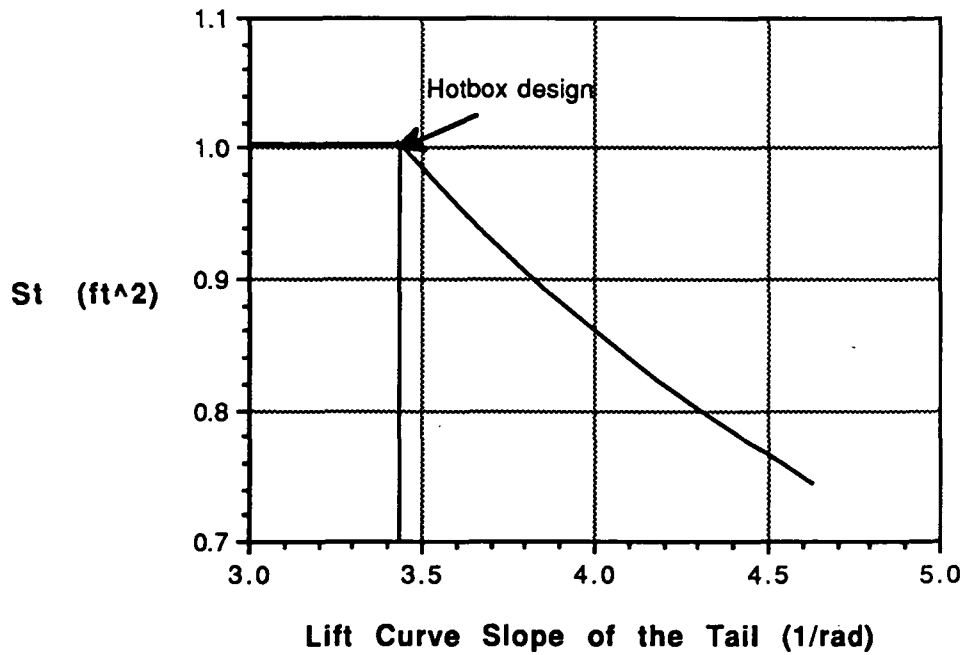## Horizontal Tail Area vs Tail Lift Curve Slope

Figure 5.3 Horizontal Tail Area vs. Tail Lift Curve Slope.

Only $C_{L\alpha}$ values for symmetric airfoils and the flat plate were considered since it is desirable to have the same variation in lift coefficient for a negative deflection of the elevator as for a positive deflection since both positive and negative deflections occur during flight. Even though the flat plate produces more drag than the symmetric airfoil sections, it was chosen because of the ease of construction. $C_{l\alpha}$ for an infinite flat plate was assumed to be 2π from ideal flow. This value was corrected for a finite plate using:

$$a = \frac{a_0}{\left(\frac{1+a_0}{(\pi ARe)}\right)}$$

Where a_0 is the lift curve slope of the infinite plate and a is the lift curve slope of the finite plate. The aspect ratio has a significant influence on both $C_{L\alpha t}$ and weight. As the aspect ratio decreases, so does the lift coefficient of the tail and the weight. To have a low weight and have a reasonable $C_{L\alpha t}$, the aspect ratio of the tail was set equal to 3.0. Because of the rectangular planform of the tail surface, e is approximately 0.80.

The horizontal tail area establishes the $C_{L\alpha}$ of the aircraft from the equation given earlier in the discussion on static margin. Once this is known, the moment coefficient curve for the aircraft can be shifted up or down by choosing different values for C_{mo}. The effect of the tail incidence angle on the moment coefficient curve is shown in Figure 5.4.

Because it is necessary for the aircraft to trim at cruise, C_{mo} should be chosen such that C_m of the aircraft is zero at the cruise angle of attack. C_{mo} is determined from the tail incidence angle and the following equation:

$$C_{mo} = C_{mow} + C_{mof} + \eta V_h C_{L\alpha t}(e_0 + i_w - i_t)$$

Moment Coefficient vs Fuselage Angle of Attack varying Tail Incidence Angle
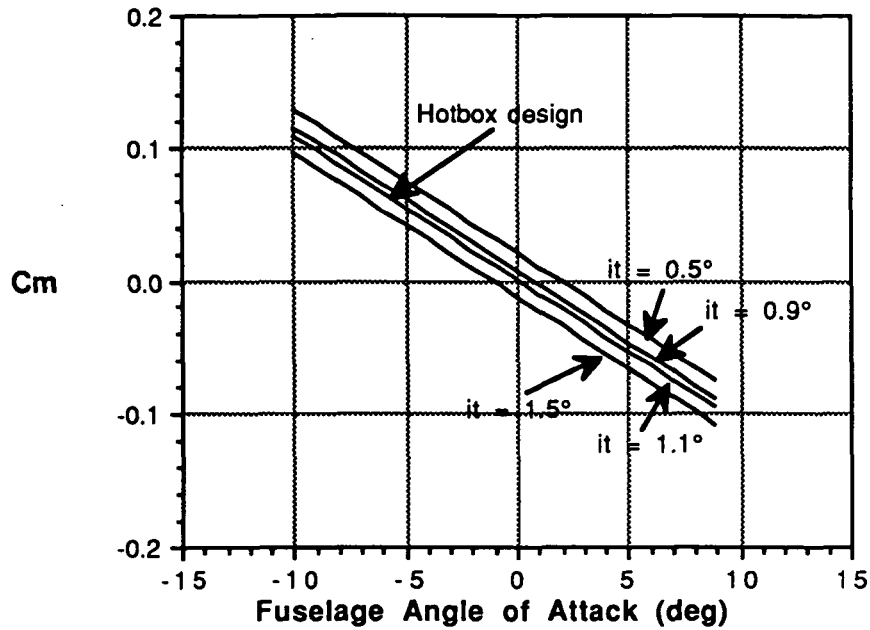
Figure 5.4 Moment Coefficient vs. Fuselage Angle of Attack at Different Tail Incidence Angles

Where C_{mow} is known from wing data, C_{mof} is given by:

$$C_{mof} = \frac{(k_2-k_1)}{36.5Sc} \sum [w_f^2(a_{ow}+i_f)\Delta x]$$

The quantity (k_2-k_1) is a function of the fuselage fineness ratio and can be determined from Figure 2.11 in Reference [5]. e_0 is given by:

$$e_0 = \frac{2C_{Lw}}{\pi AR_w} - \frac{2C_{L\alpha w}}{\pi AR_w}$$

This term corrects for the downwash from the wing. Because

$$C_m = C_{mo}+C_{m\alpha}\alpha$$

and the cruise angle of attack is known, the required C_{mo} is known. Therefore, it is a straight forward calculation to find i_t.

Shown in Figure 5.5, center of gravity location has a significant influence on the tail incidence angle.

Tail Incidence Angle vs Center of Gravity Location
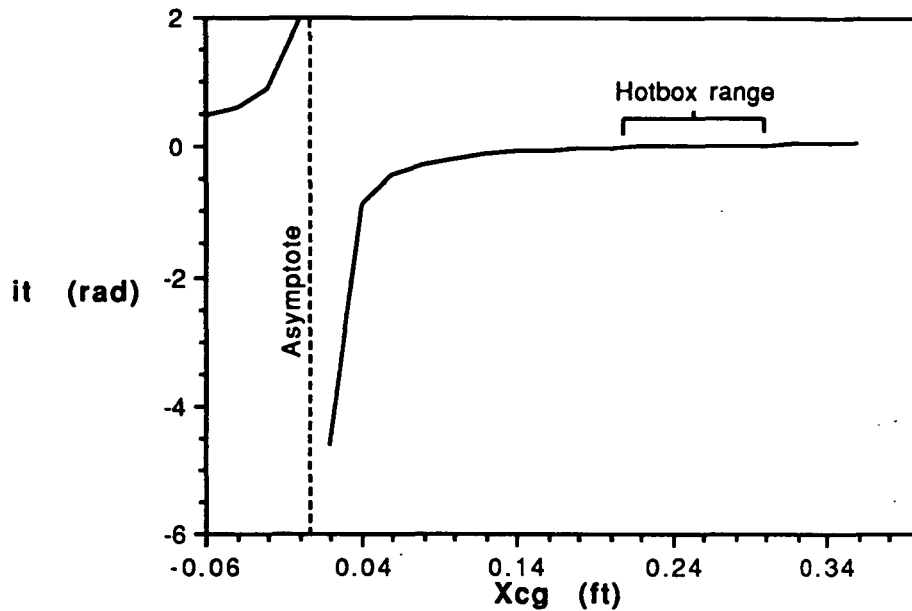
Figure 5.5 Tail Incidence Angle vs. Center of Gravity Location.

However, over the range of center of gravity locations expected for the *Hotbox*, the tail incidence angle is not greatly influenced by center of gravity travel.

The final design values for the Hotbox are:

Horizontal Tail Area, S_t	1.005 ft^2
Length to the Horizontal Tail, l_t	3.679 ft
Aspect Ratio, AR_t	3.0
Incidence Angle, i_t	1.1 °
Center of Gravity Location, x_{cg}/c	0.21-0.30
Lift Coefficient of Tail, $C_{L_{\alpha t}}$	3.43 1/rad

Table 5.1 Design Values of the Horizontal Tail

5.4 Longitudinal Control

It is necessary to control the pitching moment during a flight in order to rotate to get off the ground, climb to the desired cruise altitude, maintain level flight, descend, flair at landing, and trim at various speeds and center of gravity locations. The pitching moment control is accomplished by the use of an elevator on the horizontal tail. The elevator for the Hotbox was designed to enable the aircraft to perform a full-stall landing with the center of gravity at its forward-most location. This means that the aircraft will be capable of generating a moment by full deflection of the elevator to stall the aircraft. Slightly less deflection will enable the pilot to trim the aircraft just below the stall lift coefficient. With the addition of the elevator, the moment coefficient is given by:

$$C_m = C_{mo} + C_{m\alpha}\alpha + C_{m\delta e}\delta_e$$

where δ_e is the elevator deflection. Because the maximum elevator deflection should be able to stall the aircraft, this equation can be solved by attempting to trim the aircraft just above the stall angle. $C_{m\delta e}$ can be determined by setting $C_m=0$ and using an angle of attack just above the stall angle with the maximum elevator deflection. The effect of the elevator deflection on moment coefficient is shown in Figure 5.6.

Once $C_{m\delta e}$ is known, the elevator effectiveness, $dC_{Lt}/d\delta_e$, can be determined from:

$$C_{m\delta e} = \frac{-V_h\eta dC_{Lt}}{d\delta_e}$$

Effect of Elevator Deflection on Angle of Attack
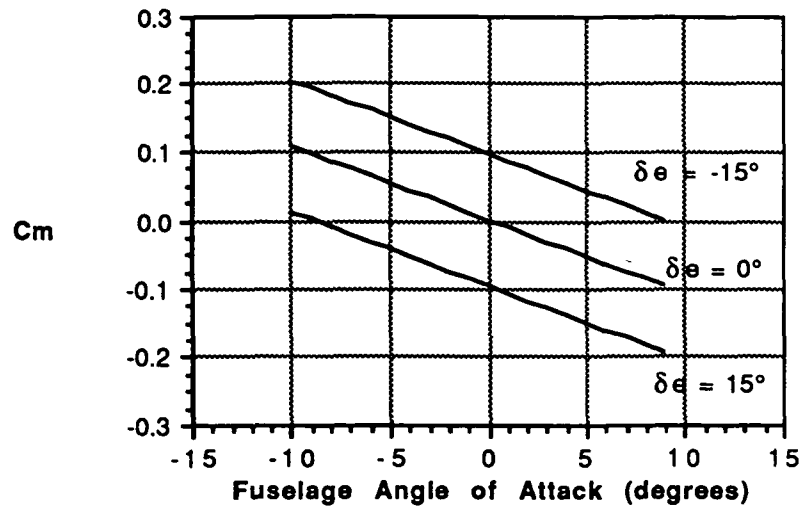
Figure 5.6 Effect of elevator on Moment Coefficient

The flap effectiveness parameter, τ, can then be determined from:

$$\frac{dC_{Lt}}{d\delta_e} = C_{L\alpha t}\,\tau$$

The flap effectiveness parameter corresponds to the ratio of control surface area to lifting surface area. The ratio of control surface area to lifting surface area can be read from Figure 2.20 in Reference [5]. The variation of moment coefficient with elevator deflection is shown in the accompanying figure. The final design parameters for the elevator of the *Hotbox* are:

$\delta_{e\,max}$	+/- 15°
$C_{m\delta e}$	0.3687 1/rad
S_e/S_t	0.09

Table 5.2 Final Design for the Elevator

5.5 Lateral Stability

Directional stability is needed by the airplane to keep a straight course or to maneuver. For the aircraft to have directional stability, the airplane must be able to resume a trim condition from some form of yawing disturbance. The yawing moment coefficient as a function of sideslip angle, β, can be written by combining equations 2.80 and 2.81 in Reference [5]. This relation is:

$$C_{n\beta} = \frac{(L_v S_v C_{l\alpha v}(0.735+1.53\frac{S_v}{S}))}{(Sb)}$$

Using this equation, the sensitivity of the yawing moment coefficient to the length of the vertical tail, the area of the vertical tail, and the lift coefficient of the vertical tail was examined. Figure 5.7 plots the change in yawing moment coefficient as a function of vertical tail area.

Yawing Moment Coefficient vs. Vertical Tail Area
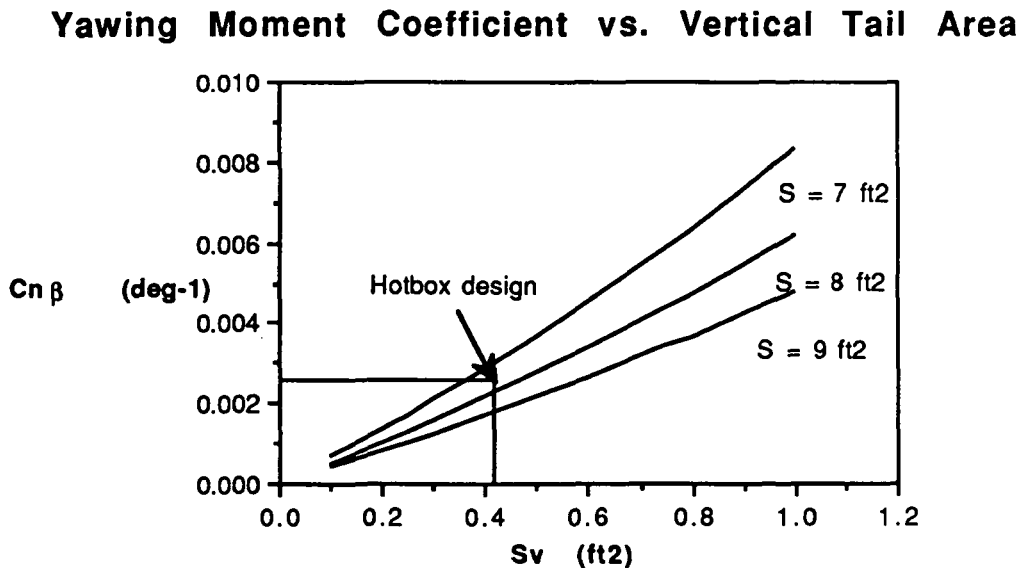
Figure 5.7 Yawing Moment Coefficient vs. Vertical Tail Area.

The graph demonstrates the dominant parabolic increase of $C_{n\beta}$ as a function of vertical tail area. Figures 5.8 and 5.9 show the yawing moment coefficient versus length to the vertical tail and the lift coefficient of the vertical tail.

Yawing Moment Coefficient vs. Length to Vertical Tail
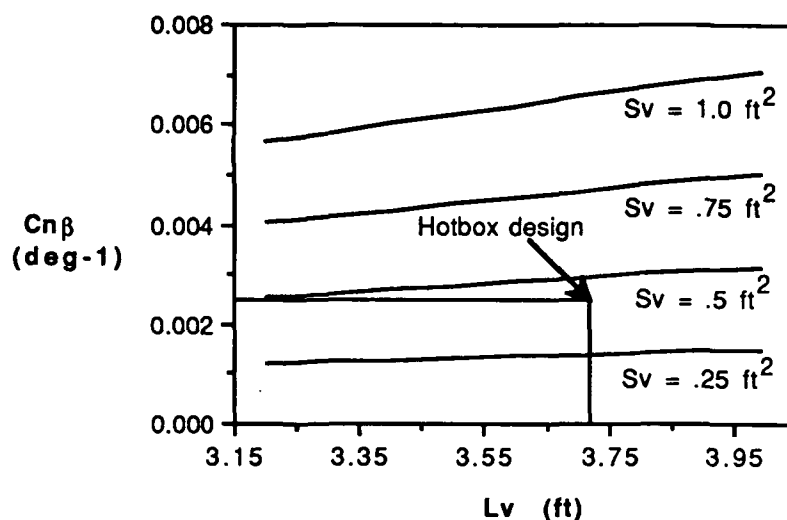
Figure 5.8 Yawing Moment Coefficient vs. Length to Vertical Tail

Yawing Moment Coefficient vs. Lift Coefficient
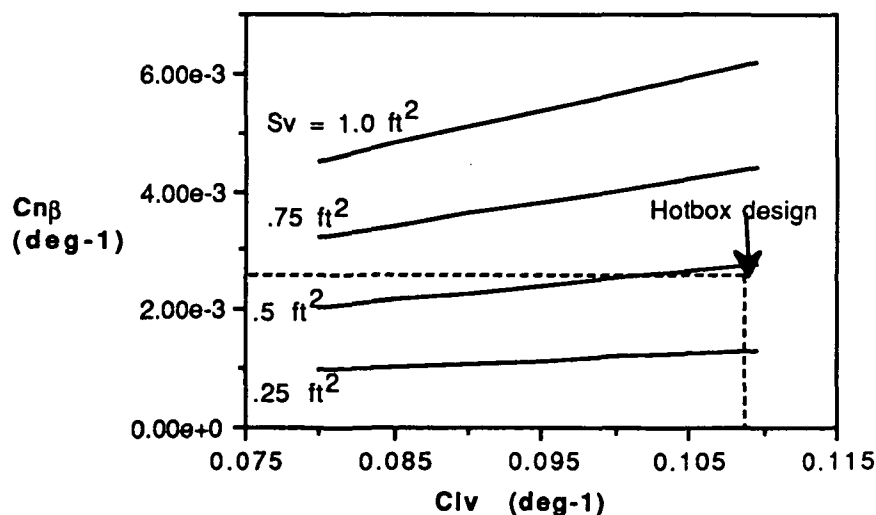
Figure 5.9 Yawing Moment Coefficient vs.Lift Coefficient of the Vertical Tail.

As can be shown from the graphs, the vertical tail area plays a more dominant role in changing the $C_{n\beta}$ than does the length to the vertical tail or changing the lift coefficient.

5.6 Lateral Control

Directional control is key requirement for airplanes. Table 2.1 in Reference [5] shows several requirements for the rudder in directional control. The chief variable in directional control is the rudder control effectiveness. By combining equation 2.86 and 2.87 in Reference [5], it is written as:

$$C_{n\delta r} = V_v \eta_v C_{l\alpha v} \tau$$

The rudder control effectiveness was examined as a function of τ, the flap effectiveness factor, and S_v, the vertical tail area. Rudder control effectiveness is plotted in Figure 5.10 versus the area of the vertical tail for four different values of τ.

Rudder Control Effectivenss vs. Vertical Tail Area

Figure 5.10 Rudder Control Effectiveness vs. Vertical Tail Area.

Even though the area of the vertical tail increases the rudder control effectiveness, the magnitude of the flap effectiveness factor is more important causing a greater increase in rudder control effectiveness.

The total yawing moment of the aircraft is a function of the yawing moment coefficient due to sideslip and the rudder control effectiveness. The equation can be written as:

$$C_n = C_{n\beta}\,\beta + C_{n\delta r}\,\delta r$$

Assuming that the turn occurs from the trim condition ($C_n=0$), the sideslip angle can be solved for by knowing the rudder deflection. The sideslip angle can then be used along with the dihedral angle to determine the rolling moment. This relation is derived in Appendix D of Reference [6] and can be written as

$$C_{l\delta r} = -0.25\,C_{l\alpha}\sin\Gamma\beta$$

This equation was examined as a function of dihedral angle, flap effectiveness factor and vertical tail area. Figure 5.11 shows the rolling moment coefficient at two different areas and two different flap effectiveness factors.

Rolling Moment Coefficient vs. Rudder Deflection Angle (Dihedral 6 degrees)
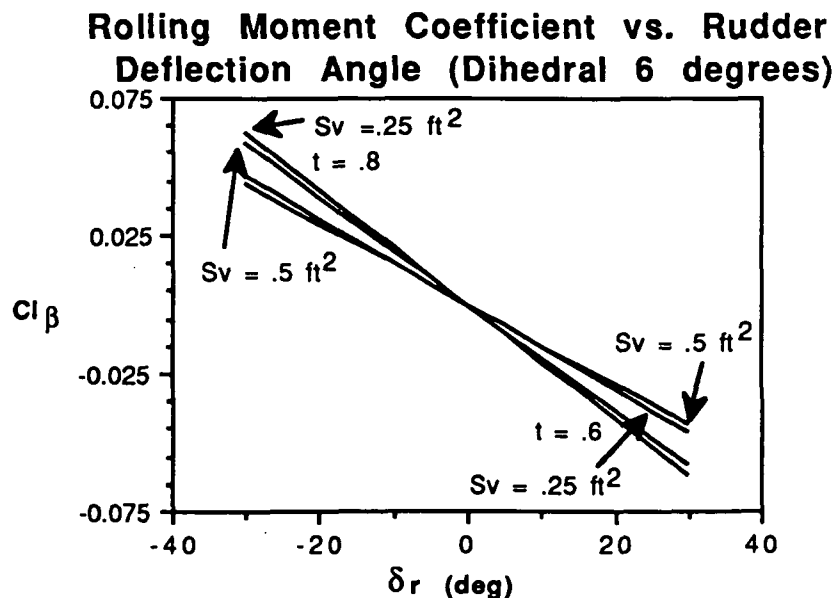
Figure 5.11 Rolling Moment Coefficient vs. Rudder Deflection

As can be seen by the graph, the rolling moment coefficient is effected more by a change in flap effectiveness factor than by changing the vertical tail area. In Figure 5.12, the rolling moment coefficient is plotted versus changes in dihedral and flap effectiveness factor.

Roll Coefficient vs. Rudder Deflection (Varying Diheral Angle)
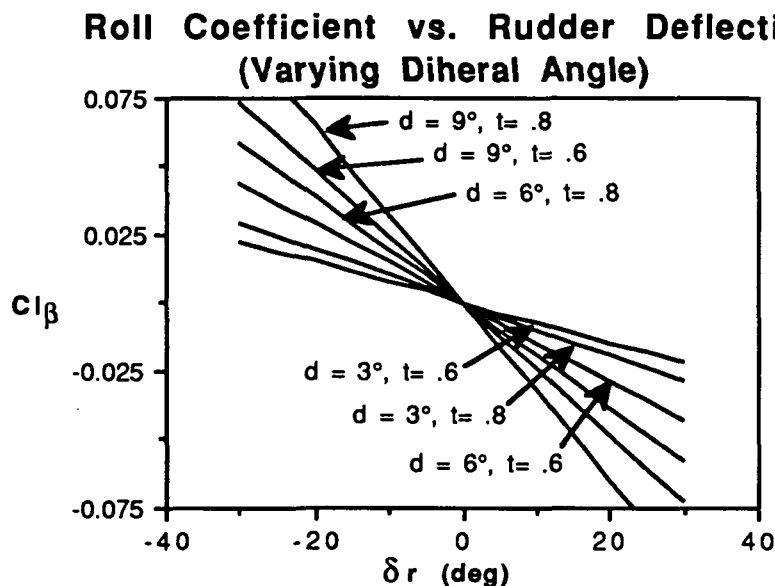
Figure 5.12 Rolling Moment Coefficient vs. Rudder Deflection (Varying Dihedral)

Both variables are dominant in the expression. A slightly greater increase in the slope of $C_{l\beta}$ occurs for an increase in flap effectiveness factor than increasing the dihedral.

In the final decision, the above analysis was examined for important trends. Most notably, the directional stability coefficient is dominated by the size of the vertical tail. The flap effectiveness factor is dominant in the rudder control effectiveness, and the rolling moment coefficient. In R/C Model Airplane Design (Reference [7]), the author recommended a 7-8°

dihedral for a mid-wing aircraft with only rudder-elevator control, an aspect ratio of 2.5 to 3 based on the formula

$$A_e = 1.55 \times A_v$$

where A_e is the effective aspect ratio and A_v is the aspect ratio of the vertical tail, and a rudder deflection of $+/-30\,°$. The *Hotbox* was designed:

Vertical Tail Area, S_v	0.42 ft^2
Aspect Ratio, A_e	2.6
Rudder Deflection, δ_r	$+/-20\,°$

Table 5.3 Final Design Parameters of the Vertical Tail

The flap effectiveness factor of the vertical tail was approximately 0.7. The values of the lateral control coefficients are given below:

Directional Stability Coefficient, $C_{n\beta}$	$2.50 \times 10e\text{-}3\ (\deg^{-1})$
Rudder Control Effectiveness, $C_{n\delta r}$	$2.20 \times 10e\text{-}3\ (\deg^{-1})$
Rolling Moment Coefficient, $C_{l\beta}$	$-2.03 \times 10e\text{-}3\ (\deg^{-1})$

Table 5.4 Lateral Coefficients

Finally, Figure 5.13 is a plot of the change in angle of attack due to the dihedral angle and yaw angle.

Change in Angle of Attack vs. Yaw Angle (Varying Dihedral)
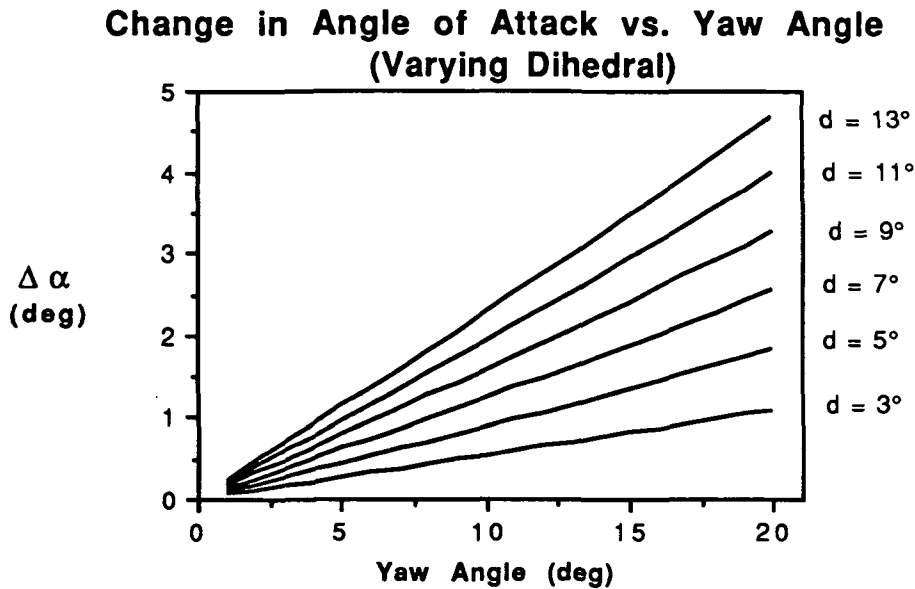
Figure 5.13 Change in Alpha vs. Yaw Angle (Varying Dihedral)

As the wing rolls, the dihedral angle in conjunction with the rudder create a yawing angle which induces a change in lift on the wing. The relationship between these three factors is given by

$$\Delta\alpha = \arctan(\sin\beta\tan\Gamma)$$

As stated earlier, the maximum rudder deflection is +/- 20 °, and the induced yaw angle will be less than the rudder deflection. Values up to 20° are plotted on the graph. The maximum dihedral plotted is 13° and at a yaw angle of 20° changes the angle of attack about 4.5°. Since our wing is mounted at approximately 5°, even this maximum change in angle of attack is below the stall value of the wing and consequently the airplane will not stall out in flight for turning.

6. PERFORMANCE

Throughout the design process it was important to ensure that the aircraft being assembled on paper was capable of meeting the design requirements established at the beginning of the design process. Performance estimates were routinely made to verify that design decisions which had been made were not jeopardizing completion of the mission requirements. Once the design was completed, final performance calculations were made for each of the phases of flight and are summarized in the table below.

Summary of Performance Characteristics

Takeoff Velocity	25.5 ft/s
Takeoff Distance	26.5 ft
Takeoff Thrust	2 lbs
Battery Drain (takeoff)	4.64 mah
Minimum Velocity	6 ft/s
Maximum Velocity	55 ft/s
Stall Speed	20.5 ft/s
Maximum R/C	10 ft/s
Maximum (L/D)	11.2
Maximum Range	20606 ft
Maximum Endurance	14.31 min.
Cruise (L/D)	10.5
Cruise Range	17000 ft
Cruise Endurance	10 min.
Turning Radius	48 ft @ 30° Bank
Landing Distance	56.6 ft

Table 6.1 Summary of Performance Characteristics

6.1 Takeoff

The ability of a propeller to allow the *Hotbox* to takeoff over a wide range of lift coefficients, weights, and battery voltages was desirable in the event of errors in construction which could result in off design performance. The selected propeller must however, meet the takeoff distance requirement of 60 ft. This length will allow us to takeoff from 13 out of the 15 cities in Aeroworld and all the cities in our targeted market. The maximum current drawn at takeoff cannot exceed 20 amps without damage to the motor. Finally, sufficient battery charge must be left to successfully complete the other phases of the mission, such as, cruise. With these requirements specified, evaluation of The *Hotbox* followed.

The Fortran code written by Prof. S. Batill, Takeoff Perf., computed the performance characteristics for takeoff given detailed propeller performance data. The program assumes fixed altitude and full throttle conditions. Due to uncertainties, an estimate of rolling friction coefficient of 0.2 was used. A summary of the design parameters used as input as well as the pertinent output is included as Table 6.2.

Input:

Weight	4.5 lbs
Planform Area	7.33 ft^2
C_L - Takeoff	0.80
C_D - Takeoff	0.0399
Prop. Diameter	1.0 ft
Battery Voltage	10.8 V
K_T (constant from motor specifications)	1.084
K_V (motor constant from specifications)	.00079
and the propeller Thrust Coefficient, C_t, and Power Coefficient, C_p, as a function of the Advance Ratio.	

Output:

Takeoff Velocity	25.5 ft/s
Time to Takeoff	2.25 s
Takeoff Distance	26.5 ft
Battery Drain	4.64 mah
Takeoff Thrust	1.99 lb
Current Draw	8.40 amps
Max Motor Power	130.90 watts

Table 6.2 Summary of Input and Output Data for Takeoff Performance Program

The takeoff performance analysis performed indicates that the *Hotbox* will satisfy all takeoff requirements.

6.2 Rate of Climb

The plot of power available and power required vs. velocity for the Top Flight (TF) 12-6 are shown in Figure 6.1. The power available curve is plotted for the full throttle condition. Results indicate that V_{min}=6 ft/s and V_{max}=55 ft/s. The *Hotbox* stalls at 20.5 ft/s, which indicates that the aircraft can never fly at the predicted minimum velocity of 6 ft/s. Finally, at 26 ft/s, a maximum rate of climb of 10 ft/s can be achieved which will allow the *Hotbox* to reach its cruise altitude of 20 ft in 2 secs.

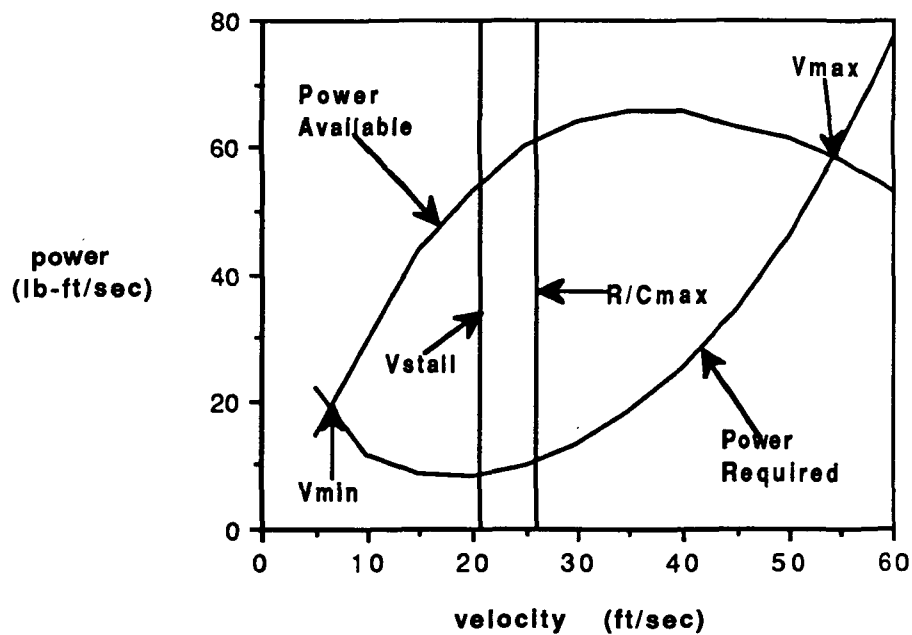## Power Required and Available v. Velocity

Figure 6.1 Power Available and Required vs Velocity

6.3 Flight Extremes

With the TF12-6, the *Hotbox* reaches its maximum lift to drag ratio (=11.2) travelling at 24 ft/s. This provides a maximum aircraft range of 20,606 ft and an endurance at that range of 14.31 mins. However, since the cruise velocity is 30 ft/s, the lift to drag ratio will decrease slightly to 10.5 and consequently range and endurance will decrease to 18,000 ft and 10 minutes, respectively. Nevertheless, use of the selected propulsion system (Astro 15, 10.8V, 1200 mah, & TF12-6) will enable the *Hotbox* to fly well over its minimum cruise range of 5500 ft. This will allow multiple flights without the expense of a battery change.

6.4 Range Considerations

The aforementioned range of 18000 ft. is the range that could be expected if the aircraft flew the entire mission at a constant velocity. That is, it does not take into account any safety estimations on reserve fuel, takeoff battery loss, and other miscellaneous battery losses which can be expected during the mission. To ensure passenger safety, the *Hotbox* will, after landing, retain 10% of its initial 1200 mah of battery power. This will allow for multiple attempts at a landing should the pilot be unable to land on first approach. Calculations using the Takeoff Perf., program have estimated a 5 mah battery drain on takeoff. In addition, Theta Group has estimated another 75 mah for ground handling, taxi (before takeoff and after landing), runway delays, redirection due to take off in a direction other than the desired flight path, and loiter. It is believed that, based on the battery drain for takeoff, this is an acceptable amount. These reductions in available battery power leave the *Hotbox* with 1000 mah for cruise. This battery power results in a flight

range of approximately 17000 ft. A summary of this information is provided in Table 6.3.

Original Battery Capacity	1200 mah
Safety Batt. Reserve	-120 mah (=10%)
Takeoff Drain	-5 mah
Misc. Battery Losses	-75 mah
Battery Left For Cruise	1000 mah

Table 6.3 Summary of Battery Losses

6.5 Range vs. Payload

Pertinent in the performance analysis of a commercial transport aircraft is an investigation into how far the aircraft can transport different payloads. This information, contained in a Range / Payload diagram, allows for immediate determination of the cruise range which can be expected given the payload weight. The Range vs. Payload diagram below (Figure 6.2) was constructed using the Battery Power Left For Cruise (=1000 mah) so it gives the cruise range as discussed earlier. As previously mentioned, for the design payload of 4.5 lbs (fully loaded aircraft), the *Hotbox* can be expected to fly 17000 ft in cruise. In the event of an empty flight (no passengers, weight=4.26 lbs), the Hotbox can be expected to cruise to a distance of 17250 ft.
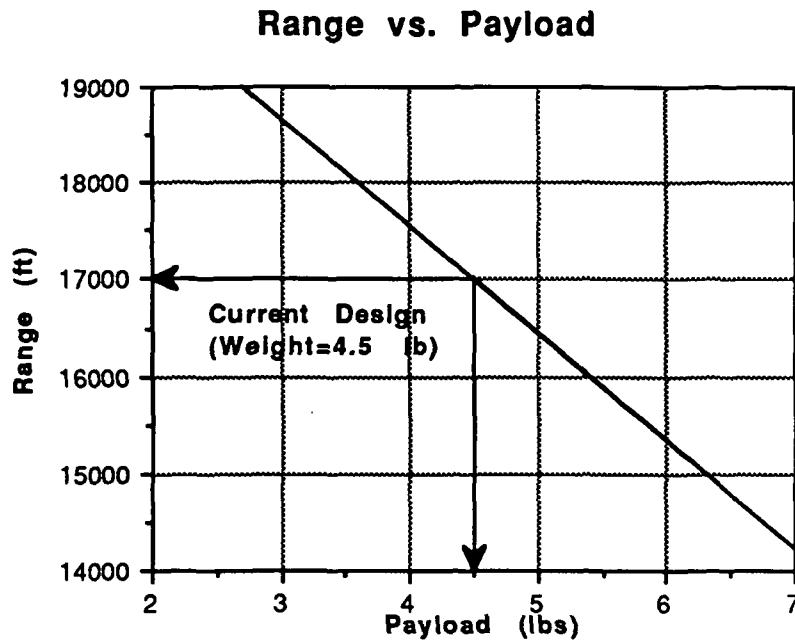
Range vs. Payload

Figure 6.2 Range vs. Payload

6.6 Turning Flight

In examining the turning performance of the aircraft, the main requirement was to be able to negotiate the turn within the requirements of the mission definition. The Hotbox will be required to negotiate a steady level turn with a maximum radius of 60 ft. The chief parameter in the steady level turn was the bank angle (ϕ), or the related load factor, n. The relationship between the two parameters is:

$$n = \frac{1}{\cos (\phi)}$$

Figure 6.3 shows the load factor on the aircraft for bank angles up to 40°.

Load Factor vs. Bank Angle
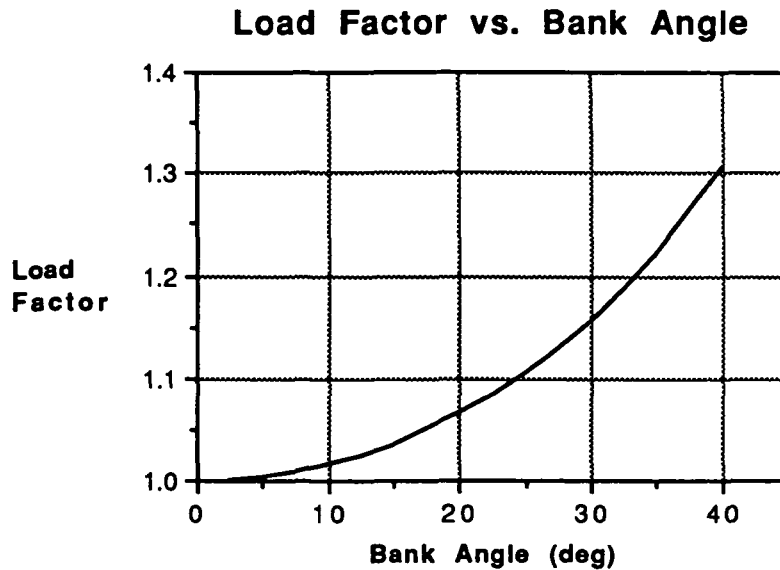
Figure 6.3 Load Factor vs. Bank Angle

As can be seen from the figure, the load factor increases with increasing bank angle. The load factor limit of 2 is not reached. This trend is important because of structural considerations on the aircraft, although in the case of this figure, the loads on the structure are less than the limitations set by the structural design.

The turn radius in a steady level turn can be mathematically written as:

$$R = \frac{V^2}{g * \tan(\phi)}$$

Figure 6.4, plots the turn radius as a function of bank angle for three different velocities.

Turn Radius vs. Bank Angle (Varying Speed)
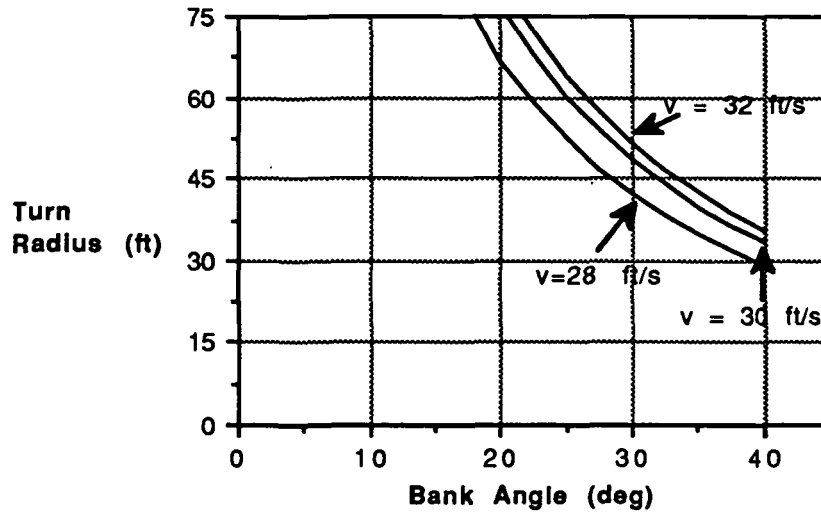
Figure 6.4 Turn Radius vs. Bank Angle (Varying Speeds)

The relationship is particularly sensitive to bank angle, while showing a weak sensitivity to the velocity term. The lower limit for the turn was set using the maximum turning radius of 60 feet which was imposed by the course. This radius corresponds to a bank angle of 25°. The upper limit for the turn was set at a bank angle of 35°. This limit was set mainly for passenger comfort during the turn.

The lift coefficient required to maintain the turn was calculated and plotted in Figure 6.5.

Lift Coefficient vs. Bank Angle
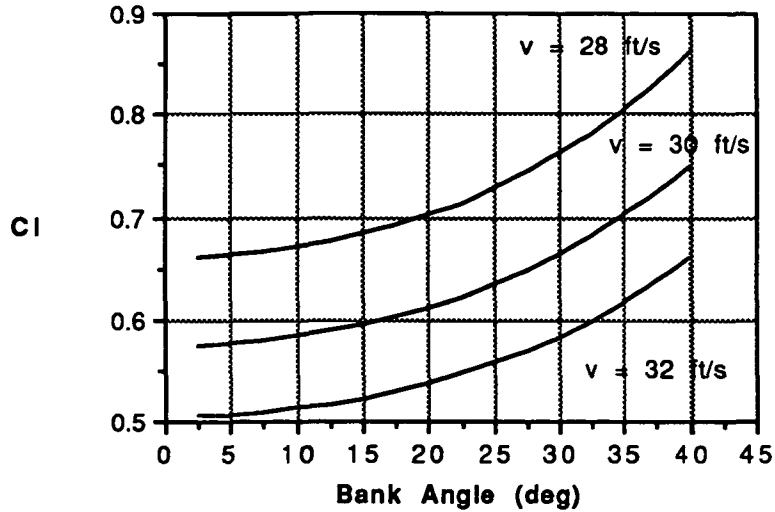
Figure 6.5 Lift Coefficient vs. Bank Angle

The mathematical relationship is:

$$C_l = \left\{ \frac{W}{S} \frac{1}{q\cos(\phi)} \right\}$$

Since $\cos(\phi)$ remains large over the bank angles under consideration, this parameter presented only minimal concern over generating additional lift. At a velocity of 30 ft/s and bank angle of 30°, the lift coefficient need only be increased by 0.05. This additional lift can be produced by throttling up on the engine during the turn, without adversely effecting the aircraft performance.

Using the equations 5.5 and 5.7 of Reference [5], the steady state roll rate was determined. The equation can be written as:

$$P_{ss} = \frac{-2u_oC_{l\delta r}\Delta\delta r}{C_{lp}\, b}$$

The steady state roll rate for the aircraft came out to approximately 25.4°/s at full rudder deflection. It will take 1 sec to reach the bank angle for maximum turn radius and will take longer than 1 second to reach larger values of bank angle.

For the *Hotbox*, the turn radius is targeted at a bank angle of 30° which is a turn radius of 48.4 feet.

6.7 Landing

Landing estimates were found using J.D. Anderson's approximation from <u>Introduction to Flight</u> (Reference [8]), p.313:

$$X_{land} = \frac{1.69W^2}{g\rho SC_{l_{max}}[\, D + \mu(W-L)]}$$

Although not obvious in the equation, velocity is a pertinent quantity in the equation (within the calculations for Lift, Drag, and $C_{l_{max}}$) and is not equivalent to the cruise velocity. Anderson suggests:

$$V_t = 1.2V_{stall}$$

$$V_{land} = 1.2V_{stall}$$

This results in a landing distance of 57 ft. This distance falls well within the maximum landing distance of 75 ft.

The performance analysis conducted on the Hotbox has confirmed that the aircraft selected in the design process will meet or exceed all of the performance requirements as established in the Design Requirements and Objectives.

Appendix 1 REQUEST FOR PROPOSALS

A.1.1 Commercial Air Transportation System Design

Commercial transports operate on a wide variety of missions ranging from short 20 minute commuter hops to extended 14 hour flights which travel across oceans and continents. In order to satisfy this wide range of mission requirements "families" of aircraft have been developed. Each basic airplane in the family was initially designed for a specific application but from that basic aircraft numerous derivative aircraft are often developed. The design of the basic aircraft must be sensitive to the fact that derivative aircraft can be developed.

Though they may differ in size and performance, all commercial designs must also possess one common denominator; they must be able to generate a profit which requires compromises between technology and economics. The objective of this project will be to gain some insight into the problems and trade-offs involved in the design of a commercial transport system. This project will simulate numerous aspects of the overall system design process so that you will be exposed to many of the conflicting requirements encountered in a systems design. In order to do so in the limited time allowed for this single course a "hypothetical world" has been developed and you will be provided with information on geography, demographics and economic factors. The project is formulated in such a fashion that you will be asked to design a basic aircraft configuration and derivative aircraft which will have the greatest impact on a particular market. The project will not only allow you to perform a systems design study but will provide an opportunity to identify those factors which have the most significant influence on the system design and design process. Formulating the project in this manner will also allow you the opportunity to fabricate the prototype for your aircraft and develop the

experience of transitioning ideas to "hardware" and then validate the hardware with prototype flight testing.

A.1..2 Problem Statement

The project goal will be to design a commercial transport which will provide the greatest potential return on investment in a new airplane market. Maximizing the profit that your airplane design will make for your customer, the airline, will be the design goal. You may choose to design the plane for any market in the fictitious world from which you believe the airline will be able to realize the most profit. This will be done by careful consideration and balancing of the variables such as the number of "passengers" carried, range/payload, fuel efficiency, production costs, and maintenance and operation costs. Appropriate data for each is included later.

The "world" market in which the airline will operate is shown in Figure A-1. Table A-1 gives the number of people who wish to travel between each possible pair of cities each day. Table A-2 gives other useful information regarding each city: details on location, runway length (Length=factor * 75 ft) and number of gates available to your airline and their size. The up-start airline may operate in any number of markets provided that they use only one airplane design and its derivatives. Consider derivative aircraft as a possible cost-effective way of expanding its market.
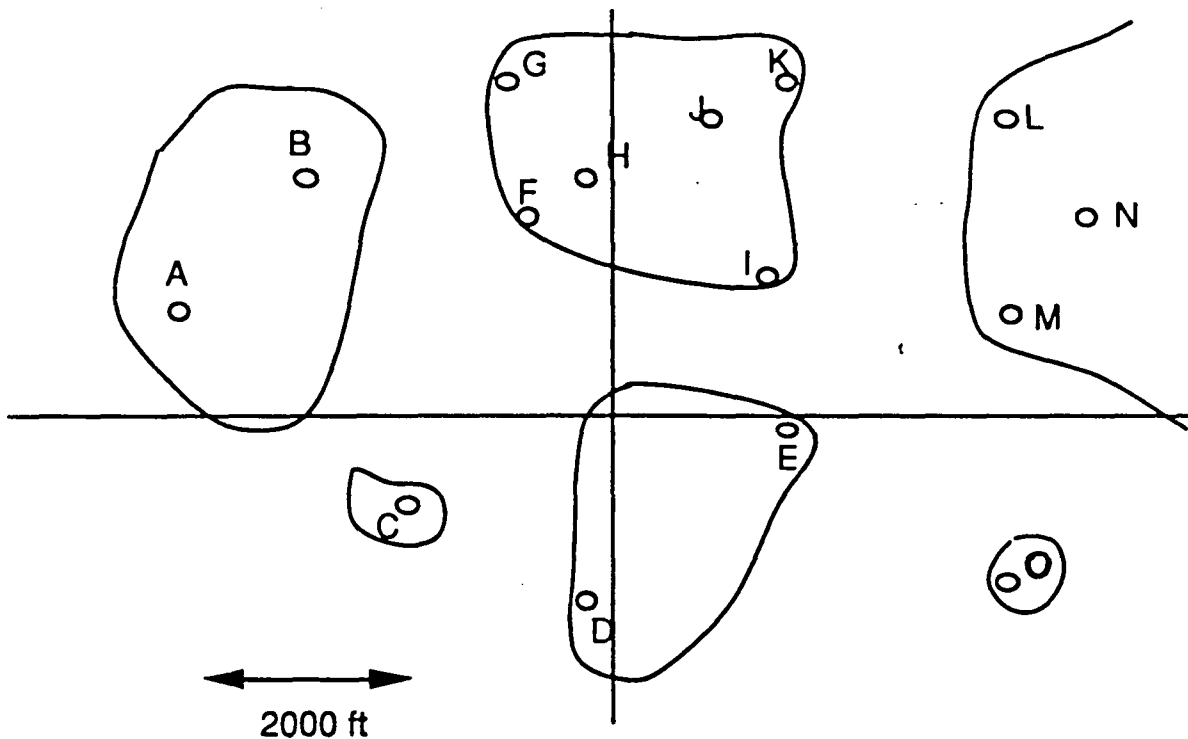
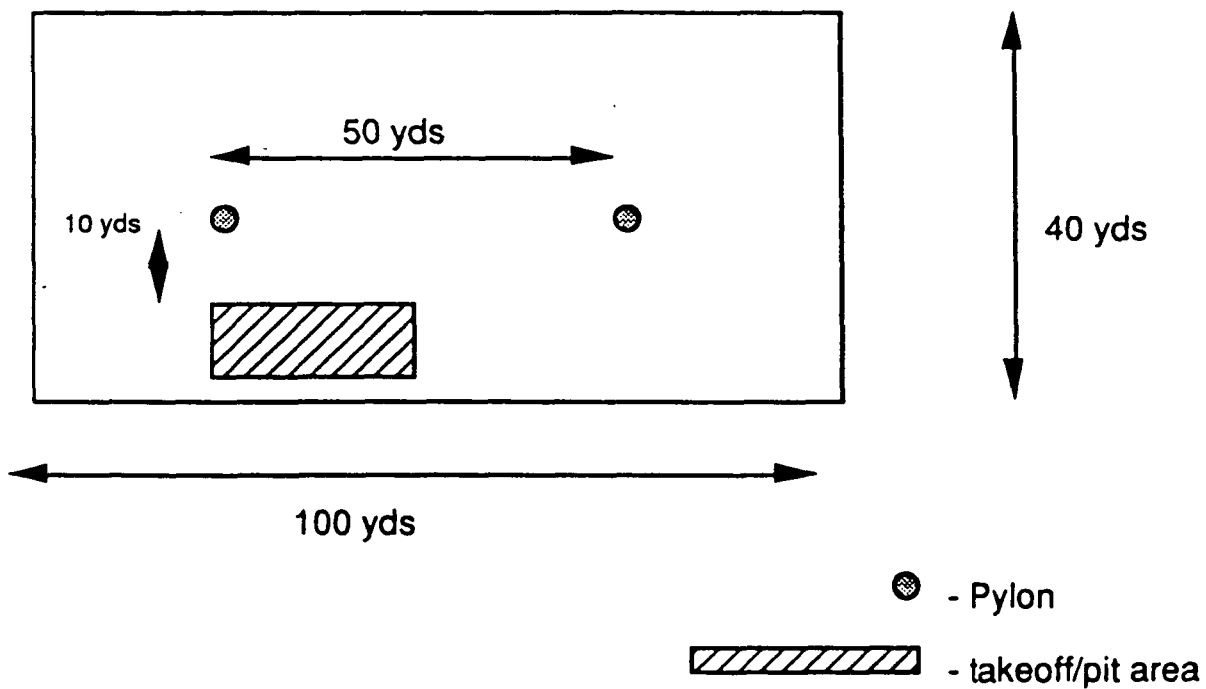FIGURE 1: "AERO-WORLD" GEOGRAPHY

FIGURE 2: PROTOTYPE FLIGHT TEST

CITY	A	B	C	D	E	F	G	H	I	J	K	L	M	N	O
A	0	500	200	20	20	200	350	40	100	300	350	80	60	80	20
B	500	0	100	20	20	350	400	60	150	400	400	400	100	200	20
C	200	100	0	30	20	120	90	30	30	30	50	300	30	20	20
D	20	20	30	0	150	60	40	30	90	60	80	30	20	20	20
E	20	20	20	150	0	100	30	20	200	100	200	60	30	30	20
F	200	350	120	60	100	0	350	60	250	400	500	250	200	250	20
G	350	400	90	40	30	350	0	300	300	300	250	200	150	120	20
H	40	60	30	30	20	60	300	0	200	250	250	100	100	200	20
I	100	150	30	90	200	250	300	200	0	350	450	250	200	200	20
J	300	400	30	60	100	400	300	250	350	0	500	300	250	300	20
K	350	400	60	80	200	500	250	250	450	500	0	400	450	500	20
L	80	400	300	30	60	250	200	100	250	300	400	0	350	400	20
M	60	100	30	20	30	200	150	100	200	250	450	350	0	350	20
N	80	200	20	20	30	250	120	200	200	300	500	400	350	0	20
O	20	20	20	20	20	20	20	20	20	20	20	20	20	20	0

TABLE 1. DAILY PASSENGER LOAD

CITY	LONG.	LAT.	Runway Length factor	# of Gates available - Gate size
A	-21	6	1	2-5ft, 1-7ft
B	-15	12	0.8	3-5ft, 2-7ft
C	-10	-5	0.6	2-5ft, 1-7ft
D	-1	-10	1	2-5ft
E	9	-1	1	5-5ft, 3-7ft
F	-4	10	1	5-5ft, 2-7ft
G	-5	17	1	4-5ft, 2-7ft
H	-1	12	1	2-5ft, 1-7ft
I	8	7	1	3-5ft, 1-7ft
J	5	15	1	5-5ft, 2-7ft
K	9	17	1	4-5ft, 2-7ft
L	20	15	1	4-5ft, 2-7ft
M	20	5	1	3-5ft, 1-7ft
N	24	10	1	4-5ft, 1-7ft
O	20	-9	0.5	1-5ft

TABLE 2. CITY INFORMATION   (Each Longitude and Latitude increment is 400 ft.)

A.1.3 Requirements

1- Develop a proposal for an aircraft and any appropriate derivative aircraft which will maximize the return on investment gained by the airline through careful consideration and balance of the number of passengers carried, the distance traveled, the fuel burned, and the production cost of each plane. The greatest measure of merit will be associated with obtaining the highest possible return on investment for the airline. You will be expected to determine the "ticket costs" for all markets in which you intend to compete. The proposal should not only detail the design of the aircraft but must identify the most critical technical and economic factors associated with the design.

2- Develop a flying prototype for the system defined above. The prototype must be capable of demonstrating the flight worthiness of the basic vehicle and flight control system and be capable of verifying the feasibility and profitability of the proposed airplane. The prototype will be required to fly a closed figure "8" course within a highly constrained envelope. A basic test program for the prototype must be developed and demonstrated with flight tests.

A.1.4 Basic information for "Aeroworld"

The following information is to be used to define special technical and economic factors for this project. Some are specific information, others are ranges which are projected to exist during the development of this airplane. [Note: real time is referred to as RWT, Aeroworld time as AWT.]

1. Passengers: Standard Ping-Pong balls - Remember these are "passengers" not cargo, therefore items like access, comfort, safety, etc. are important.

2. Range: distance traveled in feet

3. Fuel: battery charge in milli-amp hours (RWT)

4. Production cost = $400 per dollar spent on the prototype + $100 per prototype construction man-hour (RWT)

5. Maintenance (timed battery exchange) = $500 per man-minute (RWT)

6. Fuel cost = $60-$120 per milli-amp hour (RWT)

7. Regulations will not allow your plane to produce excessive "noise" from sonic booms; consider the speed of sound in this "world" to be 35 ft/sec.

8. The typical runway length at the city airports is 75 ft, this length is scaled by a runway factor in certain cities.

9. Time scale is 1 minute RWT = 30 minutes AWT

10. The world has uniform air density to an altitude of 25 ft and then is a vacuum.

11. Propulsion systems: The design, and derivatives should use one or a number of electric propulsion systems from a family of motors provided by the instructor.

12. Handling qualities: To be able to perform a sustained, level 60 ft radius turn.

13. Loiter capabilities: The aircraft must be able to fly to the closest alternate airport and maintain a loiter for one minute AWT.

14. There are two existing modes of transportation in Aeroworld which offer competition to your market:

> An average train fare costs $6.25 per 50 ft + $50 flat rate
> An average ship fare costs $8.00 per 50 ft + $65 flat rate

A.1.5 Special considerations

The prototype system will be an RPV and shall satisfy the following:

1. All basic operation will be line-of-sight with a fixed ground based pilot, although automatic control or other systems can be considered.

2. The aircraft must be able to take-off from the ground and land on the ground under its own power.

3. The prototype flight tests will be conducted within a restricted altitude range of a figure "8" course with a spacing of 150 ft between the two pylons which define the course. The flight tests for the Technology Demonstrator will be conducted in the Loftus Center on a closed course. The altitude must not exceed 25 ft at any point on the course.

4. The complete aircraft must be able to be disassembled for transportation and storage and fit within a storage container no larger than 2'x3'x5'.

5. Safety considerations for a systems operations are critical. A complete safety assessment for the system is required.

6. The Technology Demonstrator will be a full sized prototype of the actual design and must be used to validate the most critical range/payload condition for the aircraft.

7. Takeoff must be accomplished within a 75 ft takeoff region.

8. The design team must make provisions for estimating fuel burned, flight speed and distance traveled during the tests. This information is to be monitored from ground based observers.

9. A complete record of prototype production cost (materials and manhours) is also required.

10. The radio control system and the instrumentation package must be removable and a complete system installation should be able to be accomplished in 30 min.

11. System control for the flight demonstrator will be a Futaba 6FG radio system with up to 4 S28 servos or a system of comparable weight and size.

12. All FAA and FCC regulations for operation of remotely piloted vehicles and others imposed by the course instructor must be complied with.

REFERENCES

[1] James, George W.   Airline Economics. D.C. Heath and Company,
         Massachusetts, 1982

[2] Selig, Michael; Donovan, John F. and Fraser, David B.   Airfoils at Low
         Speeds. H.A. Stokely Publisher, Virginia, 1989

[3] Hoerner, Sighard. Fluid Dynamics Drag. Published by Author, New Jersey,
         1958

[4] Jensen, Daniel "A Drag Prediction Methodology for Low Reynolds
         Number Flight Vechicles", University of Notre Dame, Indiana,
         February 1990

[5] Nelson, Robert. Flight Stability and Automatic Control. McGraw Hill
         Book Company, New York, 1989

[6] Brenner, et al. "Drag-N-Fly, A Proposal in Response to a Low Reynolds
         Number Station Keeping Mission", University of Notre Dame,
         Indiana, May 1990

[7] Lennon, A.G. R/C Model Airplane Design, Motorbooks International,
         Wisconsin, 1986

[8] Anderson, John D. Introduction to Flight ,2nd edition. McGraw Hill Book
         Company, New York, 1985